ANNUAL REVIEWS

*Annual Review of Control, Robotics, and Autonomous Systems*

# Fast and Flexible Multiagent Decision-Making

Naomi Ehrich Leonard,[1] Anastasia Bizyaeva,[2] and Alessio Franci[3,4]

[1]Department of Mechanical and Aerospace Engineering, Princeton University, Princeton, New Jersey, USA; email: naomi@princeton.edu

[2]Department of Mechanical Engineering and National Science Foundation AI Institute in Dynamic Systems, University of Washington, Seattle, Washington, USA; email: anabiz@uw.edu

[3]Department of Electrical Engineering and Computer Science, University of Liège, Liège, Belgium; email: afranci@uliege.be

[4]WEL Research Institute, Wavre, Belgium

Annu. Rev. Control Robot. Auton. Syst. 2024. 7:12.1–12.27

The *Annual Review of Control, Robotics, and Autonomous Systems* is online at control.annualreviews.org

https://doi.org/10.1146/annurev-control-090523-100059



## Keywords

opinion dynamics, multiagent systems, networks, decision-making, nonlinear dynamics, bifurcation theory, tunable sensitivity

## Abstract

A multiagent system should be capable of fast and flexible decision-making to successfully manage the uncertainty, variability, and dynamic change encountered when operating in the real world. Decision-making is fast if it breaks indecision as quickly as indecision becomes costly. This requires fast divergence away from indecision in addition to fast convergence to a decision. Decision-making is flexible if it adapts to signals important to successful operation, even if they are weak or rare. This requires tunable sensitivity to input for modulating regimes in which the system is ultrasensitive and in which it is robust. Nonlinearity and feedback in the decision-making process are necessary to meeting these requirements. This article reviews theoretical principles, analytical results, related literature, and applications of decentralized nonlinear opinion dynamics that enable fast and flexible decision-making among multiple options for multiagent systems interconnected by communication and belief system networks. The theory and tools provide a principled and systematic means for designing and analyzing decision-making in systems ranging from robot teams to social networks.

## 1. INTRODUCTION

Advancing our understanding of the decision-making behavior of multiagent systems inspires challenging questions and benefits many research areas and practical applications. A fundamental and unifying question is how a large group of interacting agents makes decentralized choices that enhance performance in the presence of uncertainty and dynamically changing context even when individuals are limited in sensing, computation, and actuation. Researchers and practitioners across many areas of science, social science, mathematics, and engineering have contributed theory, methodology, experiments, and analysis to the study of opinion formation, decision-making, and the collective behavior of multiagent systems.

Examples of multiagent decision-making in engineering include safe, efficient navigation of multivehicle networks (1–3), coordination of multirobot teams for environmental monitoring (4–6), search and rescue (7–9), human–robot collaboration (10–12), decision-making and task allocation in multirobot teams (13–16), and synchronization in power grids (17–19). In biological science, examples include collective decision-making in animal groups (20–25); decision-making and phenotypic differentiation in individual cells (26); collective decision-making in groups of cells, including social microorganisms (27, 28); speciation (27, 29, 30); and the dynamics of cognitive computations in decision-making (31–35). In social science, examples include the role of social networks and social behavior in governance (36), in elections (37), in financial trading (38, 39), in international diplomacy (40), in political polarization (41–45), and in shaping public opinion on epidemics (46, 47) and climate change (48).

We define a multiagent system as a group of agents, each representing an individual or a population that makes its own decisions but can interact with, communicate with, or observe others in the group during its decision-making. A communication network, typically encoded by a graph, represents which agents observe, communicate with, or interact with which other agents. There can be other important underlying networks. For example, a belief system network, also encoded by a graph, represents logical, psychological, or social constraints on the alignment between beliefs on different options (49). There may also be an attention network that captures which agents account for which other agents' opinions in evaluating the urgency of a decision.

A central concern of this review is that a multiagent system should be capable of decision-making that is fast and flexible if it is to successfully manage the uncertainty, variability, and dynamic change encountered when operating in the real world. We call the decision-making of a multiagent system fast if it breaks indecision as quickly as indecision becomes costly. This requires fast divergence away from indecision in addition to fast convergence to a decision. We call the decision-making flexible if it adapts to signals important to successful operation, even if weak or rare, distinguishing these signals from unimportant fluctuations. This requires tunable sensitivity to inputs, i.e., parameters or "dials" in the system for modulating regimes in which the system is ultrasensitive (necessary for flexibility) and in which the system is insensitive (necessary for robustness). Nonlinearity and feedback are necessary to meet these requirements. Analytical tractability is necessary to provide rigorous and systematic prediction of the role of network structure and other parameters.

**Figure 1** shows evidence of fast and flexible decision-making by two multiagent systems: the formation of a consensus by a honey bee swarm for the best nest site (**Figure 1*a***) (50) and the polarizing ideological positions of Republicans and Democrats in the US Congress from 1959 to 2019 (**Figure 1*b***) (43). The honey bee swarm makes a fast decision starting just before 11:00 (as seen in piping), with flexibility to changing conditions verified in Reference 50. House-hunting honey bees demonstrate flexibility too in their ability to break deadlock when there is little or no evidence distinguishing a pair of alternatives (51) (see Section 5.2). Sharp changes in the

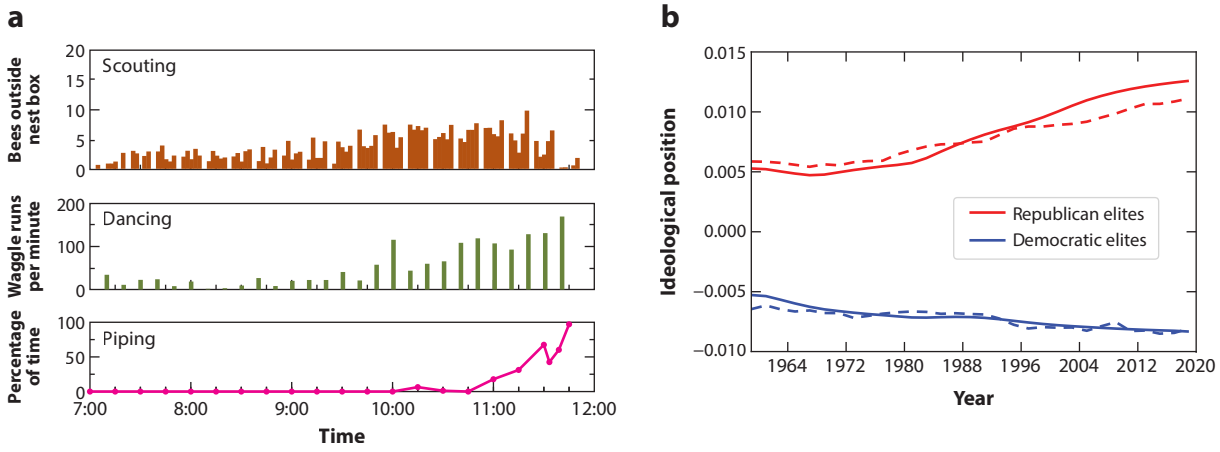


**Figure 1**

(*a*) A honey bee swarm choosing a nest site among five candidate sites. Scouts accumulate evidence, waggle dance to advertise, and pipe to alert nonscouts that a decision has been made. (*b*) Changing ideological position measured by DW-NOMINATE (Dynamic Weighted Nominal Three-Step Estimation) scores averaged across members of US Congress (*dashed lines*) and by model prediction (*solid lines*). Panel *a* adapted from Reference 50 with permission from *American Scientist*, magazine of Sigma Xi, The Scientific Research Honor Society; panel *b* adapted from Reference 43.

Republican ideological position can be explained by a model of fast and flexible decision-making but not by linear dynamics (43) (see Section 7).

Motivated by compelling evidence from the literature, we model multiagent decision-making as a dynamical, nonlinear process organized by bifurcations, controlled by feedback, and modulated by network structure. The dynamical process is the coupled evolution over time of each agent's real-valued decision states, defined as each agent's opinions and each agent's attention, which we represent as a gain on the agent's observations of its own and other agents' opinions. We focus on the evolution of opinions and attention in continuous time, but a parallel story can be derived in discrete time.

Nonlinear dynamics are distinguished from linear dynamics in that they exhibit bifurcations and can be studied through bifurcation theory (52–54). A (local) bifurcation is a change in the number and/or stability of equilibrium solutions of a nonlinear dynamical process as a (bifurcation) parameter varies across a critical value. The critical value and the point in state space where the change in equilibrium solutions happens define the bifurcation point. At a bifurcation point, the linearization of the dynamics has at least one eigenvalue with zero real part—i.e., there is a singularity in the dynamics. The associated right null eigenspace is the critical subspace that determines the bifurcation center manifold, along which the bifurcation continues. The associated left null eigenspace is the sensitivity subspace that determines the sensitivity of the bifurcation to additive input.

Near bifurcation, the process is selectively ultrasensitive to input. This means the process is both responsive to even very small signals, provided they excite the dynamics along the critical subspace, and robust to even very large signals, provided they do not excite these dynamics. Away from bifurcation, there can be multiple stable solutions that are robust to small uncertainty and perturbation. Nonlinear behaviors organized by bifurcations can be very fast in the sense that transitions between solutions can be switch-like. How and when transitions occur can be controlled and tuned by feedback, e.g., if a bifurcation parameter evolves as a function of the state.

**Bifurcation theory:** the study of qualitative changes in properties (e.g., number and stability of equilibria) of a smooth dynamical system as a function of parameters or input

**Critical subspace:** the right eigenspace of the Jacobian at the bifurcation point associated with bifurcating (purely imaginary) eigenvalues

**Center manifold:** the low-dimensional set in a dynamical system state space in which the qualitative changes associated with a bifurcation happen; it is tangent to the critical subspace at bifurcation

**Sensitivity subspace:** the left eigenspace of the Jacobian at the bifurcation point associated with bifurcating (purely imaginary) eigenvalues

**Bifurcation diagram:** a graphical display of qualitative changes in equilibrium solutions and properties of a smooth dynamical system as a function of a bifurcation parameter

In the dynamical evolution of opinions, the (average) attention is a bifurcation parameter. When attention is lower than the bifurcation value, linear negative feedback dominates and the opinions linearly track inputs or biases, thus remaining stably neutral or relatively weak when such inputs or biases are nonexistent or relatively small. When attention is higher than the bifurcation value, nonlinear positive feedback dominates such that the neutral or relatively small opinions are destabilized and strong and robustly stable opinions are formed, even for nonexistent or small inputs. We call this an indecision-breaking bifurcation, because it can be understood to correspond to a bifurcation, transition, or tipping point that allows multiagent systems to break potentially costly indecision. When attention increases dynamically, the opinions change as determined by the indecision-breaking bifurcation diagram. When attention is driven by opinion-state feedback, the bifurcation transforms such that the transition from weak to strong opinions at the indecision-breaking bifurcation can be very fast as well as tunably sensitive to inputs. We show how an analytically tractable model allows derivation of the bifurcation point, critical subspace, sensitivity to input distribution, and opinion patterns, as a function of network structure.

We give an illustrative numerical example (Section 2), review theoretical principles (Section 3), and discuss equations and their interpretation (Section 4), analytical results (Section 6), and applications and extensions (Section 7) of a general model of decentralized, multiagent and multioption, nonlinear opinion dynamics that enable fast and flexible decision-making. We also review related work from the literature (Section 5): weighted averaging and consensus dynamics and variations, investigations of the indecision-breaking ability of honey bees, and well-studied computational neuroscience models for multialternative decision-making.

## 2. ILLUSTRATIVE EXAMPLE

**Figure 2** provides an illustration through simulations of the model of coupled opinion and attention dynamics presented in detail in Section 4. The simulations show opinion formation about two options for 13 agents exchanging opinions over a communication network, shown as a graph on the left. The top (bottom) graph and plots correspond to positive (negative) unit-valued network connections. Four agents receive an external input of the same strength $\bar{b} > 0$ during the time period $t \in [0.7, 0.8]$, with two agents receiving input $\bar{b}$ in favor of option 1 and two receiving input $-\bar{b}$ in disfavor of option 1. The plots in the middle (right) show the time evolution of opinion $z_{i1} \in \mathbb{R}$ of each agent $i$ about option 1 in the case $\bar{b} = 0.1$ ($\bar{b} = 0.3$). The more positive (negative) is $z_{i1}$, the more agent $i$ favors (disfavors) option 1. The system remains close to neutral ($z_{i1} \approx 0$, for all $i$) for the small input ($\bar{b} = 0.1$) but responds rapidly, strongly ($|z_{i1}| \approx 1$), and persistently to the larger input ($\bar{b} = 0.3$).

In the simulations shown in **Figure 2**, each agent increases its attention as the magnitude of its own opinion grows. Opinion exchange and feedback control of attention determine the emergence of an implicit distributed network threshold for the formation of strong opinions in response to inputs. In the middle plots of **Figure 2**, input strength $\bar{b}$ is not large enough to cross the threshold. On the right, $\bar{b}$ is large enough to cross the threshold, leading to an opinion cascade. The implicit threshold on $\bar{b}$, between 0.1 and 0.3, above which there is an opinion cascade, is tuned by several factors, including (*a*) how inputs are distributed among the agents, (*b*) the communication network topology, and (*c*) parameters of the feedback dynamics of attention. These factors determine how well aligned the input is with the bifurcation sensitivity subspace: the better the alignment, the lower the threshold.

In the top (bottom) right plot, corresponding to all positive (negative) network connections, the opinions cascade into an agreement in favor of option 1 (disagreement where some agents favor option 1 and the rest favor option 2). The cascade behavior and opinions formed are robust

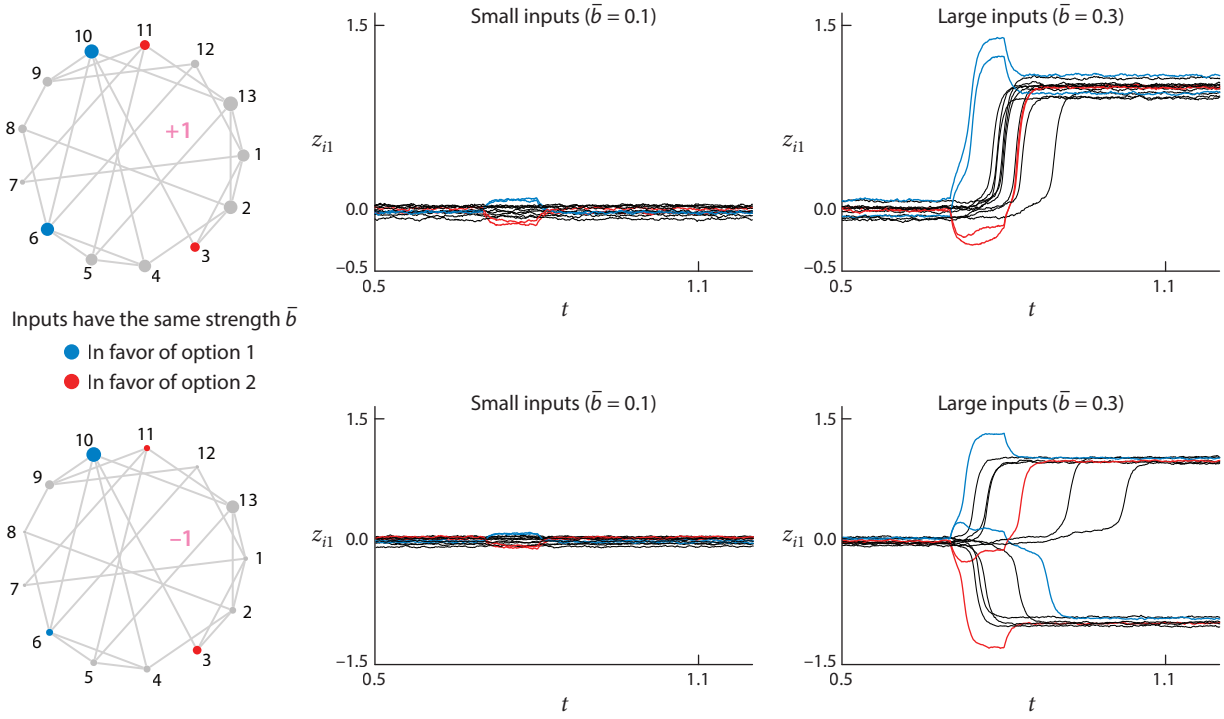


**Figure 2**

Simulated opinion and attention dynamics of Equations 3 and 4 for 13 agents and two options. The top (bottom) graphs show for every agent $i$ its opinion $z_{i1}$ of option 1 over time $t$ given the communication network graph on the left with all edges +1 (−1). Node size is scaled to the corresponding component of the leading left eigenvector of the graph adjacency matrix; larger size implies greater sensitivity to input. Input of strength $\bar{b}$ is applied only during time $t \in [0.7, 0.8]$ and only to agents 3, 6, 10, and 11.

to the small random parameter perturbations and noise added to the dynamics. Because of nonlinearity, the opinions grow much larger in magnitude than the input. Because of the multistability, the strong opinion response outlasts input presentation. Because of the networked opinion exchange, the agents receiving input do not necessarily form opinions consistent with the input they received.

These observations are predicted by the theoretical principles (Section 3) and analytical results (Sections 4 and 6). The bifurcation point, critical subspace, postbifurcation pattern of opinions, and sensitivity of behavior to the distribution of input over the network are given in terms of network structure. The results extend beyond the example of **Figure 2** to an arbitrarily large number of agents and options, mixed-sign networks, and oscillations.

## 3. THEORETICAL PRINCIPLES

### 3.1. Pitchfork Bifurcation as a Principle for Two-Option Indecision-Breaking

**Figure 3** illustrates the intimate connection between fast and flexible decision-making and bifurcation theory (52–54). The organizing bifurcation of fast and flexible decision-making between two options is the pitchfork bifurcation. **Figure 3*a*** shows the bifurcation diagrams of different instances of the pitchfork. The bifurcation parameter that drives the bifurcation is the attention $u$ that the deciding agents, on average, pay to network interactions.

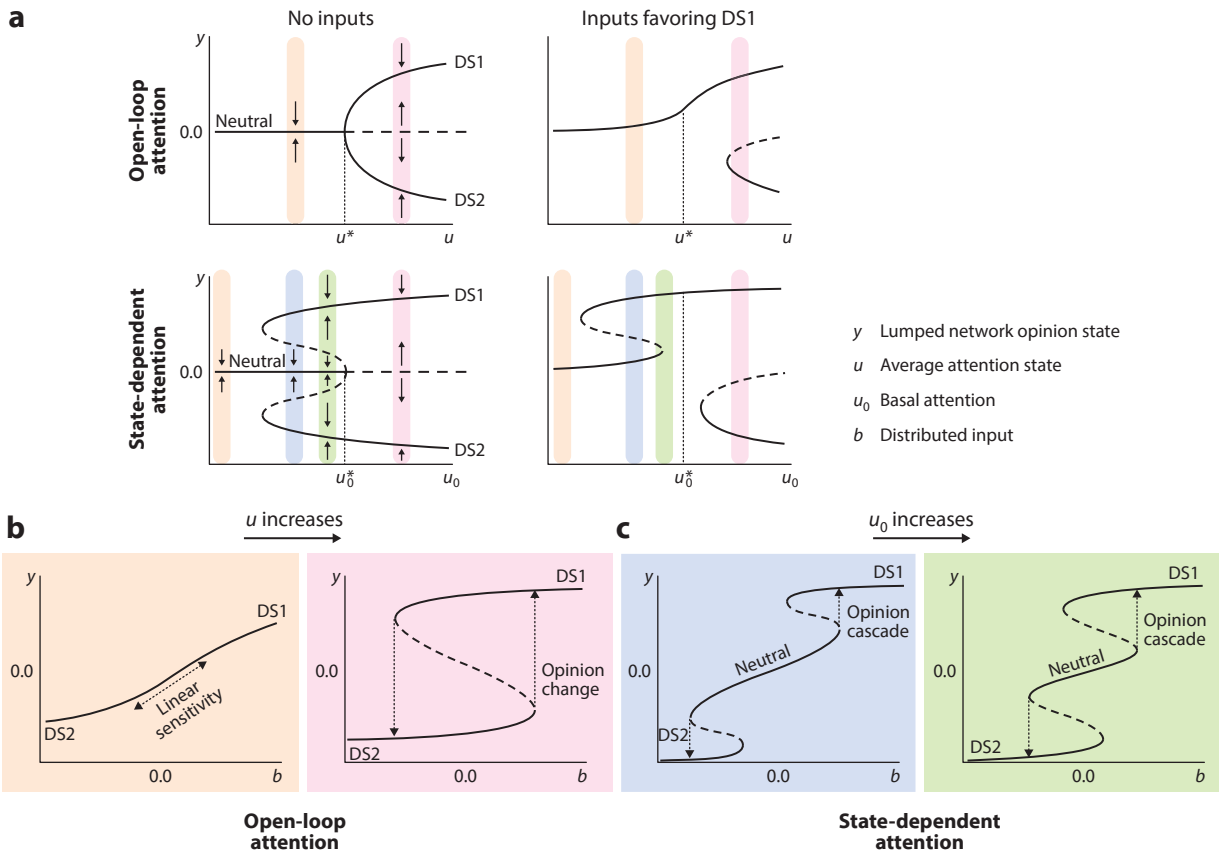


**Figure 3**

(*a*) Pitchfork bifurcation diagrams with average open-loop attention $u$ (*top*) or basal attention $u_0$ (*bottom*) as the bifurcation parameter and lumped network opinion state $y$ as the state variable. At the bifurcation point, $u = u^*$ (*top*) or $u_0 = u_0^*$ (*bottom*). Bifurcation branches of stable (unstable) equilibria are depicted as solid (dashed) lines, as graphically illustrated by the small arrows. The shaded color regions are associated with bifurcation diagrams in panels *b* and *c* that use the same colors. (*b*) Input–output bifurcation diagrams for the open-loop attention case, where the distributed input $b$ plays the role of the bifurcation parameter. (*c*) Input–output bifurcation diagrams for the state-dependent attention case. Abbreviation: DS, decision state.

**3.1.1. Breaking indecision in the absence of inputs: symmetric pitchfork.** Consider the setting with no inputs or biases and open-loop attention—i.e., changes in the agents' average attention $u$ do not depend on the agents' opinion state. As the average attention grows, the equilibrium corresponding to a neutral (indecision) state loses stability in a symmetric pitchfork bifurcation at a critical attention value $u^*$ (bifurcation point), and two new stable equilibria appear along the pitchfork bifurcation branches (**Figure 3*a***, top left).

The two new equilibria are two distinct opinionated decision states, DS1 and DS2. They can describe agent agreement: All agents favor option 1 (option 2) in DS1 (DS2). Or they can describe agent disagreement: Agents in cluster 1 favor option 1 (option 2), and agents in cluster 2 favor option 2 (option 1) in DS1 (DS2). The decision states emerging at the pitchfork are determined by the communication network structure, which shapes the bifurcation critical subspace and thus its center manifold. At the pitchfork bifurcation, the agents break indecision by choosing one decision state. Indecision-breaking occurs even without evidence (inputs or biases) distinguishing

the option quality. The pitchfork bifurcation is the mechanism through which indecision can be broken in uncertain situations.

The scalar lumped opinion state $y$ is the projection of the vector of agent opinions onto the bifurcation critical subspace. If the critical subspace corresponds to a vector with same (differently) signed elements, then $y$ is a weighted sum (difference) of agent opinions. The two decision states are described by $y > 0$ (DS1) and $y < 0$ (DS2).

**3.1.2. Breaking indecision in the presence of inputs: pitchfork unfolding and selective ultrasensitivity.** In the presence of inputs, the pitchfork unfolds, according to unfolding theory, as in the top-right bifurcation diagram in **Figure 3*a***, where the distributed input $b$ provides evidence in favor of DS1 (since $b > 0$). If the evidence were in favor of DS2 (i.e., $b < 0$), then this diagram would be flipped across the $y = 0$ axis. The distributed input $b \in \mathbb{R}$ is the projection of the vector of inputs over the network onto the sensitivity subspace of the bifurcation. A choice for the decision state favored by the inputs is a stable equilibrium for all values of $u$ and the only equilibrium for $u$ close to $u^*$. For larger $u > u^*$, a choice for the decision state disfavored by the inputs appears in a saddle-node bifurcation: Strong social interactions make a switch to the disfavored equilibrium possible.

The input-induced change in the pitchfork bifurcation diagram is a form of selective ultrasensitivity. The model is ultrasensitive at the bifurcation because its linearization is singular, and along the critical subspace the input–output gain blows up (called susceptibility in Reference 24). The directions of ultrasensitivity are determined by the dominant eigenstructure of the communication network adjacency matrix. Ultrasensitivity is selective at the bifurcation because only inputs with nonzero projection on the center manifold can excite dynamics that trigger an unfolding. The qualitative nonlinear effect of inputs on the center-manifold dynamics are predicted using Lyapunov–Schmidt reduction and unfolding theory techniques (53).

**3.1.3. Flexible and robust decision-making through the pitchfork.** For $u < u^*$, there exists a unique exponentially stable equilibrium for all values of $b$, leading to the monotone input–output characteristic in the left diagram of **Figure 3*b***. For small input, this characteristic is well approximated by a linear response. For $u > u^*$, there is bistability between the two stable decision states. Bistability implies hysteresis: Only sufficiently large changes in the input can change the decision state, as captured by the multivalued input–output characteristic in the right diagram of **Figure 3*b***. This characteristic is nonlinear, so decision states can be much larger in magnitude than the input. Hysteresis provides robustness: The existence and stability of each decision state are unaffected by small perturbations. Hysteresis provides memory: Convergence to an equilibrium depends on and retains information about the past.

To summarize, indecision-breaking through the pitchfork is simultaneously selectively ultrasensitive (at bifurcation) and robust (away from bifurcation). The balance between sensitivity and robustness is flexibly tuned by how close $u$ is to $u^*$.

**3.1.4. Indecision-breaking with open-loop attention is slow.** The pitchfork bifurcation organizing indecision-breaking for open-loop attention is called supercritical. In the supercritical pitchfork, for $u < u^*$ the only stable equilibrium is the neutral state, while for $u > u^*$ the neutral state is unstable and the two decision states are stable. When indecision-breaking results from a supercritical pitchfork, opinion strength $|y|$ is a continuously increasing function of both $u$ and $|b|$. Since the speed of opinion formation is proportional to the speed of attention and input change, opinion formation can be slow even as it is selectively ultrasensitive.

**3.1.5. Closed-loop attention makes indecision-breaking fast and leads to flexible opinion cascades.** Closing the loop between opinion and attention by making attention dependent on

**Unfolding theory:** the study of how a bifurcation diagram changes qualitatively as a function of parameters and inputs

**Dominant eigenstructure:** for a matrix, the collection of eigenvalues with largest real part and associated eigenvectors

**Lyapunov–Schmidt reduction:** a dimensionality-reduction technique to derive the qualitative properties of center-manifold dynamics close to a bifurcation point; this is similar to the center-manifold reduction but usually more tractable

opinion state introduces a source of positive feedback that sharpens the pitchfork and can make it subcritical (**Figure 3*a***, bottom left). For state-dependent attention, the bifurcation parameter is basal attention $u_0$, and the subcritical pitchfork happens at critical value $u_0 = u_0^*$. In the subcritical pitchfork, with no inputs, branches of opinionated equilibria appear for $u_0 < u_0^*$, and there is multistability of the neutral state and decision states. For $u_0 = u_0^*$, the neutral state loses stability, and the network opinion state switches to a strongly opinionated equilibrium. In the presence of input, the switch is toward the favored decision state (**Figure 3*a***, bottom right). Thus, opinion formation with state-dependent attention is fast. For slowly varying input, the network opinion and attention state diverges exponentially away from a weakly opinionated, weakly attentive state and toward a strongly opinionated, strongly attentive state.

Multistability of opinion formation with state-dependent attention leads to input–output hysteresis similarly to the open-loop case but of a new kind, as depicted in **Figure 3*c***. There are two distinct regions of hysteresis, one between each opinionated equilibrium and the neutral equilibrium. This kind of hysteresis underlies opinion cascades, in which inputs switch the network from a neutral to an opinionated state, as in **Figure 2**. The distributed network threshold for the opinion cascade corresponds to saddle-node bifurcations delimiting the two neutral-opinionated hysteresis regions. Changing the value of basal attention $u_0$ changes the neutral-opinionated hysteresis ranges. As in **Figure 3*c***, increasing $u_0$ shrinks the range in which a stable neutral equilibrium exists. For $u_0 > u_0^*$, no stable neutral equilibrium exists, leading to the standard hysteretic characteristic in the right diagram of **Figure 3*b***. Thus, basal attention modulation flexibly tunes the cascade threshold.

Opinion cascades are highly nonlinear, high-dimensional, networked dynamical behavior. Their study is tractable using a mixture of linear and nonlinear techniques. The linear analysis determines the singular directions of ultrasensitivity along which the cascade-triggering saddle-node bifurcation happens. The nonlinear analysis determines the nonlinear sensitivity of the bifurcation to parameters and inputs. These techniques are scalable to large networks of agents deciding over an arbitrary number of options.

**Hopf bifurcation:** a bifurcation characterized by a pair of complex conjugate eigenvalues crossing the imaginary axis and leading to a change in stability of an equilibrium solution and the emergence of oscillatory solutions

**Equivariant dynamical system:** a dynamical system $\dot{x} = f(x)$ that is unchanged under group $\mathbb{G}$ symmetry transformations of the state space, i.e., $(g^{-1} \circ f)(gx) = f(x)$ for all $g \in \mathbb{G}$

**Equivariant bifurcation theory:** the study of bifurcation phenomena in equivariant dynamical systems

**3.1.6. Oscillatory indecision-breaking.** When the critical subspace of the indecision-breaking bifurcation is associated with a pair of complex conjugate eigenvalues, the bifurcation is a Hopf bifurcation, and the resulting opinion-forming behavior is oscillatory.

## 3.2. Generalization to Multiple Options

The bifurcation theory for fast and flexible decision-making between two options generalizes to more than two options.

**3.2.1. Multiple indistinguishable options.** When each of a pair of options is equally likely to be chosen based on inputs or network structure, the options are indistinguishable. Deciding among indistinguishable options needs an indecision-breaking mechanism. For two options, it is the pitchfork bifurcation, which is the generic bifurcation in an equivariant dynamical system that is symmetric with respect to swapping two sets of variables. The two sets of variables that can be swapped without affecting decision-making dynamics are the agents' opinions about the two indistinguishable options. For $N_o$ options, the indecision-breaking bifurcations are predicted by equivariant bifurcation theory (55, 56) for dynamical systems that are equivariant with respect to permuting $N_o$ sets of variables: the agents' opinions about the $N_o$ indistinguishable options. These bifurcations are multibranch generalizations of the pitchfork when $N_o > 2$ (57).

**3.2.2. Multiple options interrelated through a belief system.** For multiple interrelated options, the generic indecision-breaking bifurcation is a pitchfork bifurcation. The bifurcation

critical subspace and thus the emerging opinionated decision states are jointly determined by the communication network and the belief system network. More precisely, the critical subspace of the pitchfork is a dominant eigenspace of the Kronecker product of the communication network adjacency matrix and the belief system network adjacency matrix.

**3.2.3. Input and state-dependent attention with the multiple options.** Adding inputs in either multioption case unfolds the indecision-breaking bifurcations reflective of the inputs. Making attention state-dependent makes multioption decision-making fast and with a tunable threshold for triggering opinion cascades.

**Kronecker product:** the $pm \times qn$ block matrix $A \otimes B = \begin{pmatrix} a_{11}B & \cdots & a_{1n}B \\ \vdots & \ddots & \vdots \\ a_{m1}B & \cdots & a_{mn}B \end{pmatrix}$, where $A$ is an $m \times n$ matrix and $B$ is a $p \times q$ matrix

**Network-admissible dynamical system:** a dynamical system where the dynamical relationships between the variables respect the structure of a given network

### 3.3. Model and Model-Independent Approaches to Indecision-Breaking

In Section 4, we ground our theory in a computational model and then analyze it. However, a model-independent approach is also possible (58). Such an approach relies solely on a set of empirically verifiable assumptions to make testable predictions for any model or real-world system that verifies those assumptions (or only weakly violates them). Symmetry and equivariant bifurcation theory provide powerful tools for making model-independent predictions about opinion-forming behavior given the following two basic assumptions:

1. Opinions evolve continuously in time according to a smooth dynamical system. Any (apparent) discontinuity in opinion-forming behavior is necessarily caused by bifurcation phenomena. A model does not need hard thresholds or other kinds of hybrid dynamics. Instead, switch-like behaviors associated with indecision-breaking are emergent phenomena of nonlinear dynamical systems governed by feedback and bifurcations.
2. Opinion formation is a network phenomenon. Agent valuations about options are shared, transmitted, and received through communication and belief system networks. The class of dynamical systems that can describe opinion formation is determined by the theory of network-admissible dynamical systems (59).

The predictions of the model-independent approach provide ground truths for model building. One of the ground truths is that, for indistinguishable agents and options, any model of opinion formation should be able to transition from consensus (all agents agreeing perfectly) to dissensus (agents disagreeing in such a way that on average the group is neutral) through modulation only of the extent of cooperativity among the agents. The computational model of Section 4 was designed to capture this and other model-independent ground truths. Thus, model-dependent approaches can be used to explore a broader set of contexts not captured by the model-independent approach, e.g., the presence of inputs and heterogeneous communication and belief system networks, which make agents and options distinguishable and shape opinion-forming behaviors.

## 4. FAST AND FLEXIBLE MULTIAGENT DECISION-MAKING DYNAMICS

### 4.1. Definition of Opinions, Attention, Networks, Inputs, and Biases

Consider a system of an arbitrarily large (but finite) number of agents $N_a$ making decisions about an arbitrarily large (but finite) number of options $N_o$. Let $\mathcal{V}_a = \{1, \ldots, N_a\}$ and $\mathcal{V}_o = \{1, \ldots, N_o\}$ be the sets of agents and options, respectively. For every $i \in \mathcal{V}_a$ and $j \in \mathcal{V}_o$, define $z_{ij} \in \mathbb{R}$ to be the opinion of agent $i$ about option $j$. The more positive (negative) is $z_{ij}$, the more agent $i$ favors (disfavors) option $j$. When $z_{ij} = 0$, agent $i$ is neutral or undecided about option $j$. The opinion state of agent $i$ is the vector $\mathbf{z}_i = (z_{i1}, \ldots, z_{iN_o}) \in \mathbb{R}^{N_o}$, and the system opinion state is $\mathbf{z} = (\mathbf{z}_1, \ldots, \mathbf{z}_{N_a}) \in \mathbb{R}^{N_a N_o}$. The neutral (undecided) state of the system is $\mathbf{z} = \mathbf{0}$, where $\mathbf{0}$ is the vector of $N_a N_o$ zeros. For every $i \in \mathcal{V}_a$, define the variable $u_i \geq 0$ to be the attention of agent $i$. Attention $u_i$ is a gain on opinions that agent $i$ can observe, so larger $u_i$ implies greater attention. Let $\mathbf{u} = (u_1, \ldots, u_{N_a})$.

Let $a_{ik}^{jl} \in \mathbb{R}$, for $i,k \in \mathcal{V}_a$ and $j,l \in \mathcal{V}_o$, be a network weight defined as the influence factor that the opinion of agent $k$ about option $l$ has on the opinion of agent $i$ about option $j$. A positive (negative, zero) $a_{ik}^{jl}$ means positive (negative, zero) influence. We denote the self-reinforcing weight $a_{ii}^{jj}$ by $\alpha_i^j$. This is the weight of the opinion of agent $i$ about option $j$ on itself. We assume $\alpha_i^j \geq 0$. We will introduce a separate term that represents damping of the opinion of agent $i$ about option $j$. Let $b_{ij} \in \mathbb{R}$, for $i \in \mathcal{V}_a$ and $j \in \mathcal{V}_o$, be the input to agent $i$ about option $j$, where $b_{ij} > 0$ ($b_{ij} < 0$) is input in favor (disfavor) of option $j$, and $b_{ij} = 0$ means no evidence is available to agent $i$ about option $j$. Inputs include external stimuli and internal biases. Inputs and influence factors can be state or time dependent.

When all agents share the same belief system, we can introduce two graphs to simplify the representation of influences by reducing the number of network weights $a_{ik}^{jl}$. The first is the communication network graph $\mathcal{G}_a = (\mathcal{V}_a, \mathcal{E}_a, A_a)$, which encodes communication (or sensing) among agents. $\mathcal{E}_a$ is the set of edges between nodes in $\mathcal{V}_a$, where edges are communication links and nodes are agents. An edge $e_{ik} \in \mathcal{E}_a$ means that agent $i$ observes the opinion of agent $k$. $A_a = [a_{ik}^a] \in \mathbb{R}^{N_a \times N_a}$ is the communication adjacency matrix, where $a_{ik}^a$ is the influence weight of the opinion of agent $k$ on the opinion of agent $i$.

The second graph is the belief system graph $\mathcal{G}_o = (\mathcal{V}_o, \mathcal{E}_o, A_o)$, which encodes the interdependence of options, e.g., the logical, psychological, or social constraints on the alignment or antialignment between beliefs on different options (49). $\mathcal{E}_o$ is the set of edges between nodes in $\mathcal{V}_o$, where edges are influence links and nodes are options. An edge $e_{jl} \in \mathcal{E}_o$ signifies that formation of opinions about option $j$ is affected by the opinions about option $l$. $A_o = [a_{jl}^o] \in \mathbb{R}^{N_o \times N_o}$ is the belief system adjacency matrix, where $a_{jl}^o$ is the influence weight of the opinions about option $l$ on the opinions about option $j$. As an example, consider a set of options corresponding to targets in a spatial decision-making problem. A negative (positive) edge between a pair of options corresponds to targets that are (in)distinguishable.

For every $i,k \in \mathcal{V}_a$, let $a_{ik}^u \geq 0$ be the influence factor that the strength of the opinion of agent $k$ about any option $j$ has on the attention of agent $i$. Then $A_u = [a_{ik}^u] \in \mathbb{R}^{N_a \times N_a}$ is the adjacency matrix of an attention network graph $\mathcal{G}_u = (\mathcal{V}_a, \mathcal{E}_u, A_u)$.

## 4.2. Nonlinear Multiagent Multioption Opinion and Attention Dynamics

The model describes the continuous-time updates of all opinions $z_{ij}$ and attention variables $u_i$ as a function of time $t \in \mathbb{R}_{\geq 0}$ using ordinary differential equations that define the rate of change of each variable. In simulations, small noise terms and parameter perturbations are usually included to illustrate robustness of the system behavior. We use $\dot{y}$ to denote the rate of change $dy/dt$ of a variable $y$ with respect to time $t$. A general form of the coupled nonlinear opinion dynamics and attention dynamics is the following for every $i \in \mathcal{V}_a$, $j \in \mathcal{V}_o$:

$$\dot{z}_{ij} = -d_{ij} z_{ij} + S\left( u_i \left( \alpha_i^j z_{ij} + \sum_{\substack{k=1 \\ k \neq i}}^{N_a} a_{ik}^a z_{kj} + \sum_{\substack{l \neq j \\ l=1}}^{N_o} a_{jl}^o z_{il} + \sum_{\substack{k=1 \\ k \neq i}}^{N_a} \sum_{\substack{l \neq j \\ l=1}}^{N_o} a_{ik}^a a_{jl}^o z_{kl} \right) \right) + b_{ij}, \tag{1.}$$

$$\tau_u \dot{u}_i = -u_i + u_0 + K_u \sum_{j=1}^{N_o} \sum_{k=1}^{N_a} a_{ik}^u (z_{kj})^2, \tag{2.}$$

where $d_{ij} > 0$ is a damping coefficient, $\tau_u \geq 0$ is a time constant, $u_0$ is a basal level of attention, $K_u \geq 0$ is an attention gain, and $S : \mathbb{R} \to \mathbb{R}$ is any bounded saturation function satisfying $S(0) = 0$, $S'(0) = 1$, and $S'''(0) \neq 0$. When $S$ is applied to an argument that is small or moderate in magnitude, it is treated approximately as it is. But when $S$ is applied to an argument with

large magnitude, $S$ bounds it, so the agents' sensitivity decreases as opinions become large. This has rich consequences for the robust opinion-forming behaviors captured by this model, with analytical tractability, unlike for linear consensus dynamics models and many extensions, as discussed further in Section 5.

The dynamics in Equation 1 can be interpreted as a continuous-time recurrent neural network, including finite-dimensional Wilson–Cowan dynamics (60, 61) and continuous Hopfield networks (62, 63). Equation 2 is akin to gating dynamics in neuron conductance–based models (64). Importantly, the dynamic model of Equation 1 satisfies the assumptions of Section 3 and thus captures the ground truth, i.e., the model-independent predictions. Equation 2 extends and modulates the resulting dynamical repertoire.

When $K_u > 0$, Equation 2 provides a general model of agent $i$ increasing its attention with growing strength of the opinions that it can observe, independent of agents' preferences. As an example, consider a group of agents of which some have become aware that they need to evacuate a building. These agents form opinions about which of multiple exits to use. If an agent, otherwise unaware of the need to evacuate, observes the growing activity (opinions) of these agents, then its attention grows. This activates its opinion dynamics, where it will sort out which exit to use. When $K_u = 0$ or agent $i$ observes no other agent forming an opinion, $u_i$ remains at its basal value $u_0$.

The first term on the right side of Equation 1 is a linear negative feedback term (damping), which drives $z_{ij}$ to 0, the neutral opinion, in the absence of the two other terms. The second term is the saturation of the attention-modulated weighted sum of opinions that agent $i$ observes. This is a nonlinear positive feedback term—i.e., it drives $z_{ij}$ away from 0. When there is no input, i.e., $b_{ij} = 0$, for all $i, j$, then group indecision (the neutral state $\mathbf{z} = \mathbf{0}$) is always an equilibrium. It is the balance of the negative and positive feedback terms for high enough attention that leads to an indecision-breaking bifurcation and the formation of strong opinions, even for very weak initial opinions and very weak or nonexistent input. The bifurcation is symmetric (perturbed) in the absence (presence) of input.

Inside the parentheses of Equation 1 there are four terms, modulated by the attention $u_i$ of agent $i$, that influence the opinion $z_{ij}$ of agent $i$ about option $j$. The first is the self-reinforcing term. The second is the weighted sum of the opinions of agents $k \neq i$ about option $j$, where the weights are given by the communication graph; this term models interagent opinion exchanges about option $j$. The third is the weighted sum of the opinions of agent $i$ about options $l \neq j$, where the weights are given by the belief system graph; this term models the intra-agent interactions between different option valuations according to the logic of the belief system. The fourth is the weighted sum of opinions of agent $k \neq i$ about options $l \neq j$, where the weights are products of elements in both graphs; this term models interagent interaction between different option valuations according to the logic of the belief system. By networks-of-belief theory (65), the last three are social, personal, and external dissonance, respectively.

Equation 1 can be more general as $\dot{z}_{ij} = -d_{ij}z_{ij} + S(u_i \sum_{l=1}^{N_o} \sum_{k=1}^{N_a} a_{ik}^{jl} z_{kl}) + b_{ij}$. We can also move $u_i$ outside of the saturation function $S$ and/or apply different saturation functions to the sum over agents and the sum over options. These modify the interpretation but do not affect the fundamental results.

### 4.3. Dynamics for Two Options

We first take a close look at the case of two options, $N_o = 2$. If the two options are mutually exclusive (i.e., $a_{12}^o, a_{21}^o < 0$ and an opinion in favor of option 1 can be interpreted as an opinion in disfavor of option 2), then we can focus on $z_{i1}$ and let $z_{i2} = -z_{i1}$, for all $i \in \mathcal{V}_a$, Then, the

equations for $z_{i1}$ and $z_{i2}$ decouple for every $i \in \mathcal{V}_a$, and Equation 1 becomes

$$\dot{x}_i = -d_i x_i + S\left(u_i(\alpha_i x_i + \sum_{\substack{k=1 \\ k\neq i}}^{N} a_{ik} x_k)\right) + b_i, \qquad 3.$$

where we have defined $x_i = z_{i1}$, $N_a = N$, $a_{ik} = a^a_{ik} - a^a_{ik}a^o_{12}$, $d_i = d_{i1}$, $\alpha_i = \alpha^1_i - a^o_{12}$, and $b_i = b_{i1}$. We let $A = [a_{ik}]$. In the new notation, the more positive (negative) is $x_i$, the more in favor of option 1 and in disfavor of option 2 (in disfavor of option 1 and in favor of option 2) is agent $i$. Agent $i$ is neutral (undecided) if $x_i = 0$. The neutral (undecided) system state, $\mathbf{x} = \mathbf{0}$, is always an equilibrium of Equation 3 when $\mathbf{b} = \mathbf{0}$, where $\mathbf{x} = (x_1, \ldots, x_N)$ and $\mathbf{b} = (b_1, \ldots, b_N)$. Since $|a_{ik}| = |a^a_{ik} - a^a_{ik}a^o_{12}| > |a^a_{ik}|$ and $\alpha_i = \alpha^1_i - a^o_{12} > \alpha^1_i$, mutual exclusivity between options brings a source of positive feedback akin to the toggle-switch motif of systems biology (66). Equation 2 reduces to

$$\tau_u \dot{u}_i = -u_i + u_0 + K_u \sum_{k=1}^{N} a^u_{ik} x^2_k. \qquad 4.$$

Attention adjacency matrix $A_u$ is equal to $A$ if agents update their attention using observations from the communication network. In **Figure 2**, $A_u$ is equal to $\mathcal{I}$, the identity matrix—i.e., an agent's attention grows with its own opinion. As long as $u_0 > 0$, an agent's opinion can grow through observations and input (Equation 3). Whether this leads to a cascade of strong opinions across the network depends on the distributed network threshold described in Sections 1 and 3, which in turn depends on the distribution of inputs $\mathbf{b}$, network adjacency matrix $A$, basal attention $u_0$, and attention feedback gain $K_u$.

**4.3.1. One agent, two options.** To develop intuition on the fundamental ideas of fast and flexible decision-making, we reduce Equations 3 and 4 to two scalar equations by considering one agent (individual or population) with opinion $x$ about option 1 and attention $u$:

$$\dot{x} = -dx + \tanh(ux) + b, \qquad 5.$$

$$\tau_u \dot{u} = -u + u_0 + K_u x^2, \qquad 6.$$

where $d = d_{i1}$, $u = u_i\alpha_i$, and $b = b_{i1}$. We let $S(\cdot) = \tanh(\cdot)$ without loss of generality.

We examine first the open-loop attention case, i.e., $\tau_u \to 0$ and $K_u = 0$ so that $u = u_0$. Suppose that $b = 0$ (no evidence about the options). Then, an equilibrium of Equation 5 satisfies $\tanh(ux) = dx$, which we solve graphically in **Figure 4*a***. When $(d/u) \geq 1$, there is one intersection at $x = 0$ (indecision). When $(d/u) < 1$, there are three intersections at $x = -x_*$ (favor option 2), $x = 0$ (indecision), and $x = x_*$ (favor option 1).

The linearization of Equation 5 at equilibrium $x = x_e$ is $\dot{w} = Jw$, where $w = x - x_e$ and Jacobian $J = (-d + u\,\mathrm{sech}^2(ux))|_{x=x_e}$. At $x_e = 0$, $J$ is equal to $-d + u$. Thus, $x = 0$ is exponentially stable for $u < d$ and unstable for $u > d$. For $u \leq d$, let $V(x) = x^2$ be a candidate Lyapunov function. Then, for $x \neq 0$, $\mathrm{d}V/\mathrm{d}t = 2x \cdot \dot{x} = -2dx^2(1 - \tanh(ux)/(dx)) < 0$ since $\tanh(ux)/(dx)) < 1$ for $u \leq d$. Thus, $x = 0$ is globally asymptotically stable for $u = d$ and globally exponentially stable for $u < d$. At $x = \pm x_*$, $J$ is equal to $-u(d/u - \mathrm{sech}^2(ux_*))$. The first term in the parentheses is the slope of the pink line in **Figure 4*a***, and the second term is the slope of the red curve. Near $x = \pm x_*$, the pink slope is greater than the red slope, so $J < 0$ and the equilibria $x = \pm x_*$ are exponentially stable.

This analysis reveals the indecision-breaking bifurcation, shown in the top left bifurcation diagram of **Figure 3*a***, that occurs in Equation 5, when $b = 0$, as $u$ increases through the bifurcation point $(y, u) = (0, u^*)$, where $y = x$ and $u^* = d$. The globally exponentially stable equilibrium at

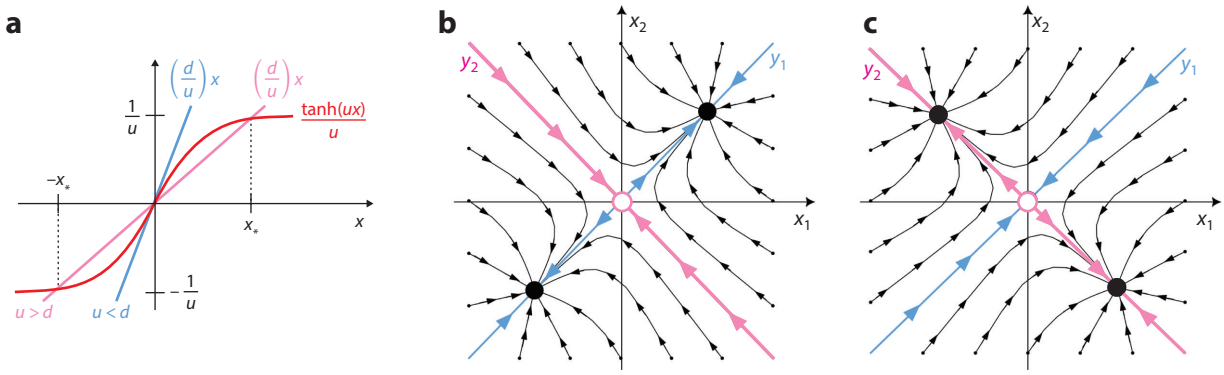


**Figure 4**

(*a*) Equilibria of the dynamics of Equation 5 for $b = 0$ and different $d/u$ ratios. When $u < d$, there exists only one equilibrium at the origin. When $u > d$, two new equilibria appear at $\pm x_*$ in a supercritical pitchfork bifurcation. (*b*,*c*) Phase planes of the dynamics of Equation 7 for $u > u^* = \frac{d}{\alpha+1}$. Panel *b* is for $A = \left(\begin{smallmatrix} 0 & 1 \\ 1 & 0 \end{smallmatrix}\right)$, and panel *c* is for $A = -\left(\begin{smallmatrix} 0 & 1 \\ 1 & 0 \end{smallmatrix}\right)$.

indecision ($x = 0$) for $u < u^*$ is destabilized for $u > u^*$, and the exponentially stable symmetric pair of equilibria, DS1 and DS2, which are a choice for option 1 ($x = x_*$) and a choice for option 2 ($x = -x_*$), respectively, grow in strength for increasing values of $u$. This is the supercritical pitchfork bifurcation. Its existence is predicted by observing that an equilibrium of Equation 5 satisfies $-dx + \tanh(ux) + b = 0$ and that, for small $|x|$, the term $-dx + \tanh(ux)$ is isomorphic to $(u - d)x - ux^3$. Thus, for $b = 0$, the equilibria of Equation 5 satisfy the normal form of the symmetric supercritical pitchfork $(u - u^*)x - ux^3 = 0$ (54), where the bifurcation happens for $(x, u) = (0, u^*)$. For $b \neq 0$, the bifurcation behavior is predicted by unfolding theory (53).

Near the bifurcation point, the dynamics are ultrasensitive to $b \neq 0$. Even for very small $|b|$, if $b > 0$, then the top left bifurcation diagram of **Figure 3*a*** unfolds into the top right bifurcation diagram, where the exponentially stable equilibrium corresponding to a choice of option 1 dominates. If $b < 0$, the diagram is flipped about the $y = 0$ line. These results are predicted by unfolding theory (53). The resulting input–output behavior for fixed $u < u^*$ ($u > u^*$) is linear (hysteretic) as in the left (right) diagram of **Figure 3*b***.

We next examine the state-dependent attention case: $K_u > 0$. The coupled opinion and attention dynamics given by Equations 5 and 6 are two-dimensional, so we can analyze them by studying their phase plane (plot of $x$ versus $u$). The nullcline of Equation 5 corresponds to $\dot{x} = -dx + \tanh(ux) + b = 0$, and the nullcline of Equation 6 corresponds to $\dot{u} = -u + u_0 + K_u x^2 = 0$. Each intersection of the nullclines corresponds to an equilibrium of the system. We illustrate the nullclines in **Figure 5*a*** for $d = 1$ and $K_u = 1$ with $b = 0.035$, $u_0 = 0.75$ (left); $b = 0.095$, $u_0 = 0.75$ (middle); and $b = 0.035$, $u_0 = 0.95$ (right). Representative trajectories are also shown, together with their time courses (**Figure 5*b***). The nullcline $\dot{x} = 0$ (in black) has the same qualitative shape in the three plots and takes the form of the top right unfolded bifurcation diagram of **Figure 3*a***. But the larger value of $b$ in the middle plots pushes the two nullcline branches farther apart as compared with those in the left and right plots. In **Figure 5*a***, the different values of basal attention $u_0$ distinguish the right plot from the two other plots: The nullcline $\dot{u} = 0$ (in gray) is the same in the right plot as in the two other plots except for a shift to the right by 0.2 (equal to $0.95 - 0.75$). This shift changes the number and location of the equilibria and, with it, the threshold above which the input is large enough to trigger the fast formation of a strong opinion. In this way, $u_0$ tunes the sensitivity of the opinion formation to the input: In the example of **Figure 5**, input $b = 0.035$ triggers a strong opinion for the high value of $u_0$ but not for the low value of $u_0$.

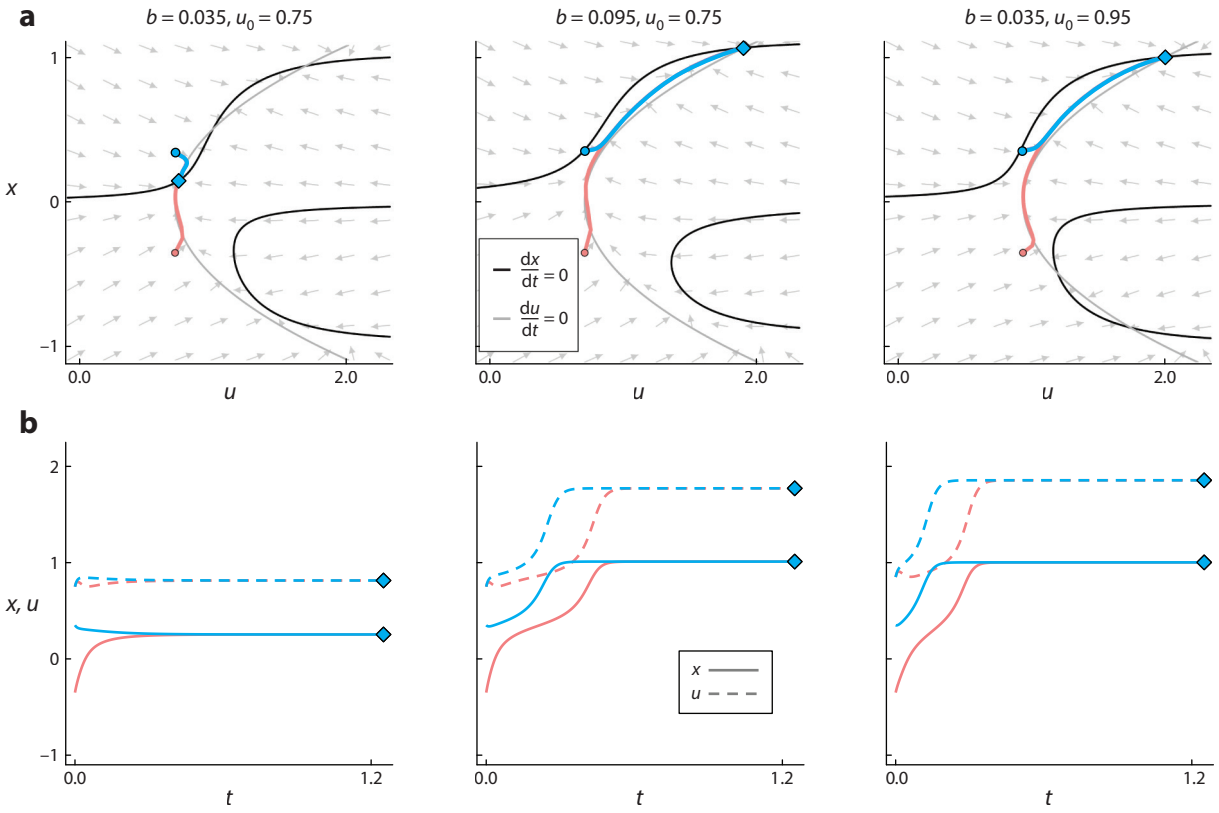


**Figure 5**

(*a*) Nullclines, vector field, and sample trajectories of the dynamics of Equations 5 and 6 for different input $b$ and basal attention $u_0$ values. The colored curves are the sample trajectories, with filled circles representing the initial conditions; the black curve is the nullcline $\dot{x} = 0$; and the gray curve is the nullcline $\dot{u} = 0$. (*b*) Time courses of the sample trajectories in panel *a*.

**Ghost of the saddle-node bifurcation:** the region in the state space close to where a saddle-node bifurcation has happened; it is associated with a slow transient converging behavior followed by a fast diverging behavior

To see this, observe in the left diagram of **Figure 5*a*** that for $u_0 = 0.75$ and $b = 0.035$, there are three equilibria (two stable and one unstable). The equilibrium near the neutral opinion is stable. Thus, solutions converge to the near-neutral equilibrium, and no strong opinion forms for either of the two initial conditions, one in favor and the other in disfavor of option 1, as can also be seen in the corresponding time plots in the left plot of **Figure 5*b***. When the input strength is increased in favor of option 1 from 0.035 to 0.095 (middle plots of **Figure 5**), the only nullcline intersection that persists is associated with a stable equilibrium corresponding to strong opinion and strong attention. The near-neutral equilibrium for $b = 0.035$ has disappeared in a saddle-node bifurcation for $b = b^*$ between 0.035 and 0.095. For the same initial conditions as the left plots of **Figure 5*a***, the trajectory is first attracted toward the ghost of the saddle-node bifurcation and then diverges exponentially away from indecision, as can also be seen in the corresponding time plots. The input strength $b^*$ for which the near-neutral equilibrium disappears is the threshold for opinion cascades. As shown in the right plots of **Figure 5**, increasing the basal attention reduces the threshold for opinion cascade. Indeed, the phase plane and temporal behavior for $b = 0.035$ and $u_0 = 0.95$ are the same as those for $b = 0.095$ and $u_0 = 0.75$. The importance of a tunable threshold is that it allows the decision-making process to tune its sensitivity and reactivity to input and a changing environment.

We can explain the fast formation of strong opinions through divergence from indecision and convergence to decision for $b > b^*$ in terms of the subcritical pitchfork bifurcation of the bottom bifurcation diagrams in **Figure 3*a***. Observe that an equilibrium of Equations 5 and 6 satisfies $-d\,x + \tanh((u_0 + K_u x^2)x) + b = 0$ and that, for small $|x|$, the term $-d\,x + \tanh((u_0 + K_u x^2)x)$ is isomorphic to $(u_0 - d)x - (K_u - u_0/3)x^3 + (K_u/3)x^5$. Thus, for $b = 0$, the equilibria of Equations 5 and 6 satisfy the normal form of the quintic pitchfork $(u_0 - u_0^*)x - (K_u - u_0/3)x^3 + (K_u/3)x^5 = 0$, $u_0^* = d$ (54), which has a subcritical pitchfork bifurcation at $(x, u_0) = (0, u_0^*)$ and a symmetric pair of saddle-node bifurcations, as shown in the bottom left bifurcation diagram of **Figure 3*a***. The stability of the various equilibria can be inferred by phase plane analysis, as in **Figure 5**, or by studying the linearized dynamics. Because the coupled opinion–attention dynamics are monotone dynamics on quadrants $x > 0$ and $x < 0$, there are no dynamical behaviors other than convergence to an equilibrium (67). For $b \neq 0$, the bifurcation behavior is predicted by unfolding theory (53). The input–output behavior is as in **Figure 3*c***, characterized by hysteresis between neutrality and decision and the existence of opinion cascades for fast, strong opinion formation. Tuning the basal attention $u_0$ shapes the input–output behavior, and we see how increasing the basal attention reduces the threshold for opinion cascades.

**Monotone dynamics:** dynamics whose trajectories satisfy a monotonicity condition with respect to some order in the state space

The single-agent analysis in this section generalizes to larger numbers of agents through the Lyapunov–Schmidt reduction. In particular, the same low-dimensional dynamics described here are found in the indecision-breaking bifurcation center manifold in higher-dimensional systems. We next work these ideas out explicitly in the case of two agents.

**4.3.2. Two agents, two options.** Consider two agents. Let $d_1 = d_2 = d > 0$, $u_1 = u_2 = u \geq 0$, and $\alpha_1 = \alpha_2 = \alpha \geq 0$, and assume a communication link with graph edge weights $a_{12} \neq 0$ and $a_{21} \neq 0$. Equation 3 becomes

$$\begin{aligned} \dot{x}_1 &= -d\,x_1 + \tanh(u(\alpha x_1 + a_{12}x_2)) + b_1, \\ \dot{x}_2 &= -d\,x_2 + \tanh(u(\alpha x_2 + a_{21}x_1)) + b_2. \end{aligned} \qquad 7.$$

Let $\mathbf{b} = \mathbf{0}$. The neutral state $\mathbf{x} = \mathbf{0}$ is an equilibrium of Equation 7 for all $u \geq 0$, and the Jacobian evaluated at $\mathbf{x} = \mathbf{0}$ is $J = (-d + u\alpha)I + uA$, where $A$ is the adjacency matrix for the two-node network. Let $\lambda_{\max}$ be a simple eigenvalue of $A$ with largest real part and $\mathbf{v}_{\max}$ and $\mathbf{w}_{\max}$ be the corresponding right and left unit eigenvectors, respectively. $J$ has largest eigenvalue

$$\lambda_1' = (-d + u\alpha + u\lambda_{\max}) = (\alpha + \lambda_{\max})(u - u^*), \quad u^* = \frac{d}{\alpha + \lambda_{\max}}, \qquad 8.$$

with right and left eigenvectors $\mathbf{v}_1' = \mathbf{v}_{\max}$ and $\mathbf{w}_1' = \mathbf{w}_{\max}$, respectively. By Equation 8, $\lambda_1'$ is equal to 0 if $u = u^* = \frac{d}{\alpha + \lambda_{\max}}$, and $\mathbf{x} = \mathbf{0}$ is exponentially stable if $u < u^*$ and unstable if $u > u^*$. We expect a supercritical pitchfork bifurcation at the critical point $\mathbf{x} = \mathbf{0}$ and $u = u^*$, with two new stable equilibria appearing for $u > u^*$ along the center manifold, which at $\mathbf{x} = \mathbf{0}$ is tangent to critical subspace $\mathrm{Ker}(J) = \mathbf{v}_1' = \mathbf{v}_{\max}$. Let $y = \langle \mathbf{x}, \mathbf{v}_{\max} \rangle$ and $b = \langle \mathbf{w}_{\max}, \mathbf{b} \rangle$.

As an example, let $a_{12} = a_{21} = 1$. Adjacency matrix $A$, its eigenvalues, and its corresponding eigenvectors are $A = \left(\begin{smallmatrix} 0 & 1 \\ 1 & 0 \end{smallmatrix}\right)$, $\lambda_1 = 1, \mathbf{v}_1 = \frac{1}{\sqrt{2}}\left(\begin{smallmatrix} 1 \\ 1 \end{smallmatrix}\right)$, $\lambda_2 = -1$, and $\mathbf{v}_2 = \frac{1}{\sqrt{2}}\left(\begin{smallmatrix} 1 \\ -1 \end{smallmatrix}\right)$. Then, $(\lambda_{\max}, \mathbf{v}_{\max}, \mathbf{w}_{\max})$ is equal to $(\lambda_1, \mathbf{v}_1, \mathbf{v}_1)$ and $u^*$ is equal to $\frac{d}{\alpha+1}$. To show the bifurcation, we compute the Lyapunov–Schmidt reduction by first rewriting Equation 7 with respect to coordinates $(y_1, y_2) = T^{-1}(x_1, x_2)$, $T = [\mathbf{v}_1, \mathbf{v}_2]$. The rows of $T^{-1}$ are the left eigenvectors $\mathbf{w}_1, \mathbf{w}_2$ of $A$, so $y_1 = \langle \mathbf{x}, \mathbf{w}_1 \rangle = \langle \mathbf{x}, \mathbf{w}_{\max} \rangle = (x_1 + x_2)/\sqrt{2}$ and $y_2 = \langle \mathbf{x}, \mathbf{w}_2 \rangle = (x_1 - x_2)/\sqrt{2}$. Denote $p_s = \alpha + 1$, $p_d = \alpha - 1$, and $\tilde{u} = u/\sqrt{2}$.

Equation 7 in the new coordinates becomes

$$\dot{y}_1 = -d\,y_1 + (1/\sqrt{2})(\tanh(\tilde{u}(p_s y_1 + p_d y_2)) + \tanh(\tilde{u}(p_s y_1 - p_d y_2)) + b_1 + b_2), \quad 9.$$

$$\dot{y}_2 = -d\,y_2 + (1/\sqrt{2})(\tanh(\tilde{u}(p_s y_1 + p_d y_2)) - \tanh(\tilde{u}(p_s y_1 - p_d y_2)) + b_1 - b_2). \quad 10.$$

Noting that $\mathbf{x} = T\mathbf{y} = y_1\mathbf{v}_1 + y_2\mathbf{v}_2$, we can restrict the dynamics of $y_1$ of Equation 9 to critical subspace $\mathrm{Ker}(J) = \mathbf{v}_1 = \mathbf{v}_{\max}$ by setting $y_2 = 0$. Since $y$ is equal to $\langle \mathbf{x}, \mathbf{v}_1 \rangle$, on the restriction, $y$ is equal to $y_1$. Using $\tanh(cx) \approx c\tanh(x)$ for small $|x|$ leads to the restricted dynamics

$$\dot{y} \approx -dy + \tanh(u(\alpha+1)y) + \langle \mathbf{w}_1, \mathbf{b} \rangle. \quad 11.$$

For small $|x|$, the right-hand side of Equation 11 is isomorphic to $(u(\alpha+1) - d)y - u(\alpha+1)y^3 + b$, $b = \langle \mathbf{w}_1, \mathbf{b} \rangle$. Thus, equilibria of Equation 11 satisfy $(u(\alpha+1) - d)y - u(\alpha+1)y^3 + b = 0$, which is the Lyapunov–Schmidt reduction and which describes, similarly to the single-agent case, a supercritical pitchfork bifurcation at $(y_1, u) = (0, u^*)$ along $\mathbf{v}_1$ when $b = \langle \mathbf{w}_1, \mathbf{b} \rangle = \langle \mathbf{w}_{\max}, \mathbf{b} \rangle = (b_1 + b_2)/\sqrt{2} = 0$. **Figure 4*b*** shows the resulting phase portrait for a choice of $u > u^*$. The top left diagram of **Figure 3*a*** shows the bifurcation diagram where $y = \langle \mathbf{x}, \mathbf{v}_{\max} \rangle = (x_1 + x_2)/\sqrt{2}$. The upper (lower) branch of the pitchfork corresponds to an agreement—consensus, in this case—of the agents for option 1 (option 2). The top right bifurcation diagram of **Figure 3*a*** corresponds to $b = \langle \mathbf{w}_{\max}, \mathbf{b} \rangle = (b_1 + b_2)/\sqrt{2} > 0$, i.e., when the distributed input (here the input average) favors option 1 (DS1).

Now suppose the weights on the communication link are $a_{12} = a_{21} = -1$. The adjacency matrix is $-A$ for which $(\lambda_{\max}, \mathbf{v}_{\max}, \mathbf{w}_{\max}) = (\lambda_1, \mathbf{v}_2, \mathbf{v}_2)$. Thus, we expect a supercritical pitchfork bifurcation at $\mathbf{x} = \mathbf{0}$ and $u = u^* = \frac{d}{\alpha+1}$, with two new stable equilibria appearing for $u > u^*$ along the center manifold, which at $\mathbf{x} = \mathbf{0}$ is tangent to critical subspace $\mathrm{Ker}(J) = \mathbf{v}_1' = \mathbf{v}_{\max} = \mathbf{v}_2$. Restricting the dynamics of $y_2 = \langle \mathbf{x}, \mathbf{w}_{\max} \rangle = \langle \mathbf{x}, \mathbf{w}_2 \rangle$ of Equation 10 to $\mathrm{Ker}(J)$ by setting $y_1 = 0$, letting $y = \langle \mathbf{x}, \mathbf{v}_2 \rangle = y_2$, and using $\tanh(cx) \approx c\tanh(x)$ for small $|x|$ gives

$$\dot{y} \approx -dy + \tanh(u(\alpha+1)y) + \langle \mathbf{w}_2, \mathbf{b} \rangle, \quad 12.$$

which describes a supercritical pitchfork bifurcation at $(y_2, u) = (0, u^*)$ along $\mathbf{v}_2$ when $b = \langle \mathbf{w}_2, \mathbf{b} \rangle = \langle \mathbf{w}_{\max}, \mathbf{b} \rangle = (b_1 - b_2)/\sqrt{2} = 0$. **Figure 4*c*** shows the resulting phase portrait for a choice of $u > u^*$. The top left diagram of **Figure 3*a*** shows the bifurcation diagram where $y = \langle \mathbf{x}, \mathbf{v}_{\max} \rangle = (x_1 - x_2)/\sqrt{2}$. The upper (lower) branch of the pitchfork corresponds to agent 1 for option 1 (option 2) and agent 2 for option 2 (option 1). The top right bifurcation diagram of **Figure 3*a*** corresponds to $b = \langle \mathbf{w}_{\max}, \mathbf{b} \rangle = (b_1 - b_2)/\sqrt{2} > 0$, i.e., when the distributed input (here the input difference $b_1 - b_2$) favors option 1 (DS1).

Now consider the state-dependent attention given by Equation 4, where $a_{ik}^u = 1$, for all $i, k = 1, 2$. Let $\mathbf{u}_{\max} = \frac{1}{\sqrt{2}}\binom{1}{1}$ and $u = \langle \mathbf{u}_{\max}, \mathbf{u} \rangle$. For illustration, suppose that $\tau_u \to 0$ such that $u_1 = u_2 = u = u_0 + K_u(x_1^2 + x_2^2)$. Substituting for $u$ in Equation 11 or 12 gives an equation locally isomorphic to the normal form for the quintic pitchfork and its unfolding of the bottom two diagrams in **Figure 3*a***. For $\tau_u > 0$, the phase planes of the top part of **Figure 5** characterize the reduced dynamics of $(y_1, u)$ in the first example and of $(y_2, u)$ in the second example. Thus, the distributed network threshold for an opinion cascade is governed by $u_0$, $K_u$, and $\langle \mathbf{w}_1, \mathbf{b} \rangle$ in the first example and $\langle \mathbf{w}_2, \mathbf{b} \rangle$ in the second example. In particular, a cascade will be triggered for a combination of sufficiently large input strength $\|\mathbf{b}\|$ and sufficient alignment of the input $\mathbf{b}$ with $\mathbf{w}_{\max}$.

**4.3.3. *N* agents, two options.** The results of Section 4.3.2 generalize to the case of $N$ agents (Equation 3) with $d_i = d$, $\alpha_i = \alpha$, and $u_i = u$, for $i = 1, \ldots N$, and adjacency matrix $A$. Suppose $A$ has simple positive leading eigenvalue $\lambda_{\max}$ with right and left leading eigenvectors $\mathbf{v}_{\max}$ and $\mathbf{w}_{\max}$, respectively. Then, $\mathbf{v}_{\max}$ defines the critical subspace and $\mathbf{w}_{\max}$ the sensitivity subspace. Following the two-agent case analysis, for $\mathbf{b} = \mathbf{0}$ there will be a supercritical pitchfork bifurcation at $\mathbf{x} = \mathbf{0}$ and $u = u^*$ where $u^*$ is defined as in Equation 8. The Lyapunov–Schmidt reduction defines dynamics of $y = \langle \mathbf{x}, \mathbf{v}_{\max} \rangle$, locally isomorphic to the normal form for the supercritical pitchfork, with $b = \langle \mathbf{w}_{\max}, \mathbf{b} \rangle$ the unfolding parameter.

A sufficient condition for the existence of a simple positive leading eigenvalue is that $A$ is an irreducible matrix or, equivalently, that it is the adjacency matrix of a strongly connected graph, and that $a_{ik} \geq 0$ for all $i, k = 1, \ldots, N$. Then the Perron–Frobenius theorem (68) implies that $A$ has the strong Perron–Frobenius property—i.e., there exists a simple positive leading eigenvalue with a positive eigenvector. Applications of Perron–Frobenius theory to more general signed networks are discussed in Section 6.

When $A$ has a simple leading eigenvalue–eigenvector triplet ($\lambda_{\max}$, $\mathbf{v}_{\max}$, $\mathbf{w}_{\max}$), the network will form opinions according to the top diagrams of **Figure 3*a*** in the open-loop attention case and according to the bottom diagrams of **Figure 3*a*** in the state-dependent attention case, where $y = \langle \mathbf{x}, \mathbf{v}_{\max} \rangle = \sum_{i=1}^{N} x_i v_i$ and $b = \langle \mathbf{w}_{\max}, \mathbf{b} \rangle = \sum_{i=1}^{N} w_i b_i$. The ordering of elements $v_i$ in $\mathbf{v}_{\max}$, the leading right eigenvector of $A$, predicts the ordering of agent opinions at steady state, i.e., steady-state opinion patterns that may involve different option preferences, different opinion strengths, and clustering of opinions. And each element $w_i$ of $\mathbf{w}_{\max}$, the leading left eigenvector of $A$, serves as a nodal centrality index for agent $i$: It predicts the relative influence of the input to agent $i$ on the network opinion formation. The higher the centrality of agent $i$ is, the greater the contribution of $b_i$ is to the distributed input $b$. Thus, inputs to nodes with high centrality are more effective in bringing the network above its distributed threshold and triggering an opinion cascade. In the example of **Figure 2**, the centrality index $|w_i|$ for node $i$ is represented by the size of the dot used to represent node $i$. Centrality indexes change with the change in network properties; for example, agent 6 has a higher influence in the top network (with edge weights equal to 1) as compared with that in the bottom network (with edge weights equal to $-1$). In the top network, the higher centrality of nodes 6 and 10, receiving input in favor of option 1, as compared with the centrality of nodes 3 and 11, receiving input in disfavor of option 1, explains why $b = \langle \mathbf{w}_{\max}, \mathbf{b} \rangle > 0$ and the group forms a consensus in favor of option 1 (for the sufficiently large input).

**Leading eigenvalues:** the eigenvalues of a matrix with largest real part; when the leading eigenvalue is unique and positive, it is also called dominant

**Leading eigenvectors:** the eigenvectors associated with leading eigenvalues

**Irreducible matrix:** a matrix that is not similar by permutation to a block upper-triangular matrix

**Strongly connected graph:** a directed graph where for every pair of nodes $i$, $k$ there is an ordered sequence of connected edges from $i$ to $k$

## 4.4. Generalization to Multiple Options

The analytical results in the case of two options generalize to more than two options when the options are interrelated but not when they are indistinguishable.

**4.4.1. Indistinguishable options.** The analysis developed above for two options does not generalize to the case of multiple indistinguishable options. The reason for this is that the symmetry of the indistinguishable options case leads to bifurcations with higher-dimensional center manifolds and Lyapunov–Schmidt reductions. Tools from equivariant bifurcation theory must thus be employed to characterize the indecision-breaking bifurcation (see 58).

**4.4.2. Multiple interrelated options.** The analysis developed above for two options can generalize to the case of multiple interrelated options. This is possible when the Kronecker product $A_a \otimes A_o$ has a simple leading eigenvalue with associated right and left eigenvectors $\mathbf{v}_{\max}$ and $\mathbf{w}_{\max}$, respectively. Then, the same results as for the two-option case (Lyapunov–Schmidt reduction,

pitchfork unfolding, and network threshold for closed-loop attention) hold for the multioption case with respect to these eigenvectors. We return to these ideas in Section 6.

## 5. CONNECTIONS TO EXISTING DECISION-MAKING DYNAMICS

### 5.1. Weighted Averaging, Consensus Dynamics, Variations, and Extensions

In his 1974 paper, Morris DeGroot (69) introduced the weighted averaging process as a model of $N$ agents coming to a consensus about the value of an unknown parameter $\theta$. In the DeGroot model, $x_i(T)$ is the opinion of agent $i$ about the unknown value at time $T$, and $x_i(0)$ is its initial estimate. The weighted averaging process is $x_i(T+1) = \sum_{k=1}^{N} \tilde{a}_{ik} x_k(T)$, where $\tilde{a}_{ik} \geq 0$ is the weight agent $i$ places on the opinion of agent $k$, and $\sum_{k=1}^{N} \tilde{a}_{ik} = 1$. Subtracting $x_i(T)$ from both sides gives $x_i(T+1) - x_i(T) = -x_i(T) + \sum_{k=1}^{N} \tilde{a}_{ik} x_k(T)$, the unit time-step Euler discretization of linear consensus dynamics in continuous time $t$:

$$\dot{x}_i(t) = -\tilde{d}_i x_i(t) + \sum_{k=1}^{N} \tilde{a}_{ik} x_k(t), \qquad 13.$$

where $\tilde{d}_i = \sum_{k=1}^{N} \tilde{a}_{ik}$ does not have to be 1, since we can always scale time. These dynamics were introduced and analyzed by Robert Abelson (70) a decade before DeGroot. Networks that yield consensus to the average of the initial condition for Equation 13 also do so for the discrete-time DeGroot model. In this sense, reaching consensus in discrete time means reaching consensus in continuous time. Linear consensus dynamics have been very well studied and applied in a range of settings (see 71–74 and references therein).

Let $\tilde{A} = [\tilde{a}_{ik}]$, $\tilde{a}_{ik} \geq 0$ and $\tilde{D} = \text{diag}(\tilde{\mathbf{d}})$. The matrix $L = \tilde{D} - \tilde{A}$ is called the Laplacian matrix associated with the network described by adjacency matrix $\tilde{A}$. Equation 13 is also $\dot{\mathbf{x}} = -L\mathbf{x}$. If the matrix $\tilde{A}$ is irreducible, then, as discussed in Section 4.3.2, by the Perron–Frobenius theorem $L$ always has a simple leading eigenvalue–eigenvector triplet ($\lambda_{\max}$, $\mathbf{v}_{\max}$, $\mathbf{w}_{\max}$), where $\lambda_{\max} = 0$, $\mathbf{v}_{\max} = \mathbf{1} = (1, \ldots, 1) \in \mathbb{R}^N$, and $\mathbf{w}_{\max}$ is a positive vector. Because all other eigenvalues are negative, all solutions of Equation 13 converge exponentially to the subspace generated by $\mathbf{v}_{\max} = \mathbf{1}$, and consensus is always reached.

Linear consensus dynamics are analytically tractable, but they are limited in capturing the breadth of real-world opinion dynamics (70, 75). First, consensus is the only solution, ruling out all other kinds of opinion formation. Second, a greater difference in opinions between an agent pair yields a stronger attraction, a paradox that does not fit our real-world experience. Third, the consensus value depends linearly on initial opinions. So small (large) initial opinions necessarily lead to small (large) final opinions. Fourth, the consensus value is independent of the graph structure, so the dynamics do not capture the greater influence that more central agents may have on the group's decision-making. Fifth, linear consensus is fragile because the zero eigenvalue implies an infinite gain (solutions diverge to infinity) with respect to constant perturbations. And sixth, linear consensus is neither fast nor flexible.

These observations have motivated variations and extensions of linear consensus dynamics. The Friedkin–Johnsen model (76, 77) introduced "stubborn" attachment of agents to their initial opinions, which admits clustering and disagreement; the model has been generalized and tested with human subjects (77–79). Jia et al. (80) combined the DeGroot model with Friedkin's model (81) of self-appraisals for opinion formation over a sequence of issues. Altafini (82) and others (83, 84) studied the linear Laplacian dynamics on signed networks. The resulting signed Laplacian dynamics can exhibit disagreement (polarized consensus) but are fragile, because if the network is not exactly structurally balanced, then all solutions converge to zero. Bounded confidence models are discontinuous models where a network weight is nonzero only when the difference in opinion between the corresponding agents is below a fixed threshold (85, 86). These models exhibit

clustering; however, analysis is usually intractable. Dandekar et al. (87) generalized DeGroot's model to account for biased assimilation, a weighted averaging process with state-dependent weights that makes the dynamics nonlinear and thus yields interesting behaviors, such as the formation of large disagreement opinions from small initial opinions (88). Mei et al. (75) proposed a weighted-median update instead of weighted averaging and showed numerically the formation of strong consensus and dissensus opinions from small initial conditions. However, the analytical tractability of both biased assimilation and weighted median models is limited.

The nonlinear opinion dynamics of Equation 3 can be viewed as a generalization of the linear consensus dynamics of Equation 13 that addresses the weaknesses of the linear model without compromising analytical tractability. The linearizations of Equation 13 at the origin for $u_i = u^* = 1$, $\alpha_i = 0$, $b_i = 0$, and $d_i = \sum_k a_{ik}$ for all $i$ are exactly the linear consensus dynamics represented by Equation 13. The saturating term in the nonlinear opinion dynamics solves the stronger-attraction-for-divergent-opinions paradox. Also, it turns the fragility of the linear consensus dynamics into the indecision-breaking pitchfork bifurcation shown in the top left diagram of **Figure 3*a***.

To see this, consider the case $a_{ik} \geq 0$ and $A$ irreducible. Then the Jacobian $J$ of Equation 3 at the neutral equilibrium and for $u_i = u^* = 1$ is exactly $L$, which has a simple leading eigenvalue $\lambda_{\max} = 0$ with right leading eigenvector $\mathbf{v}_{\max} = \mathbf{1}$. Hence, the theory summarized in Section 4.3.2 predicts a pitchfork in which the two emerging decision states are consensus states for options 1 and 2, respectively. However, consensus is not the only robust outcome of Equation 3. If the network is signed and $\mathbf{v}_{\max}$ has mixed-sign components, then the decision states are disagreement states. This is the case even when the network is far from being structurally balanced. Further, if we introduce additive inputs $b_i \neq 0$, then the pitchfork unfolds according to the distributed input $b = \langle \mathbf{w}_{\max}, \mathbf{b} \rangle$.

## 5.2. Honey Bee Decision-Making Dynamics

Seeley et al. (51) used experiments and a computational model to investigate how a swarm of house-hunting honey bees breaks deadlock (indecision) when confronted with two candidate nest sites of (near) equal value. Their experiments showed that house-hunting honey bees use the stop signal as a cross-inhibition between populations of scouts accumulating evidence for alternative candidate nest sites.

To study indecision-breaking, they derived a mean-field model of honey bee decision-making between two sites, accounting for the stop signal and activities in **Figure 1*a***. For equally valuable nest sites, the mean-field model exhibited a pitchfork bifurcation at indecision for $\sigma$, the rate of stop signaling serving as a bifurcation parameter, reaching a critical rate $\sigma^*$ (51, 89). Pais et al. (89) showed that the model behaves as predicted by bifurcation theory. They also showed that $\sigma^*$ is inversely proportional to the average nest site so that indecision is broken only if the options are of sufficiently high value. Analogous results have been worked out for a population model with $N$ options by Reina et al. (90).

The multiagent nonlinear opinion dynamics model described by Gray et al. (91) was derived to recover the tunably sensitive decision-making behavior of honey bees for a group of decision-makers communicating over a network. Their model is Equation 3 for an unsigned network and $d_i = \tilde{d}_i$, which yields consensus indecision-breaking (Section 5.1) when the average attention $u$, replacing the stop signaling rate, crosses above its critical value $u^*$.

## 5.3. Connections to Cognitive Science and Neuroscience

The opinion dynamics model of Equation 1 is directly analogous to recurrent neural networks, Hopfield neural networks (62, 63), and Wilson–Cowan networks of excitatory and inhibitory

**Stop signal:** a vibrational signal delivered as a head butt by one honey bee to another honey bee reporting on a site through the waggle dance, which causes the dancing to stop

**Hadamard product:** the $p \times q$ element-wise product $B \odot C = [b_{ij}c_{ij}]$ of two $p \times q$ matrices $B = [b_{ij}]$ and $C = [c_{ij}]$

neurons (60, 61), which are popular surrogate models for the dynamics of cognition, learning, and decision-making. Another compelling connection is with the cognitive science leaky competing accumulator (LCA) models (92–94), which encode a biologically plausible neural circuit mechanism for decision-making. Equation 1 with $a^{\mathrm{o}}_{jl} \leq 0$ is a deterministic limit of an LCA model and provides the means to rigorously generalize and extend the LCA setting to more complex belief systems and multiagent scenarios.

## 6. ANALYTICAL RESULTS ON NONLINEAR OPINION DYNAMICS

We describe the generic bifurcations supported by the opinion dynamics model. Let $u = \frac{1}{N_{\mathrm{a}}}\sum_{i=1}^{N_{\mathrm{a}}} u_i$ be the average network attention. Then the attention of agent $i$ is $u_i = u(u_i/u)$ with $u_i/u \geq 0$. Define weight parameters as $\hat{\alpha}^j_i = \alpha^j_i u_i/u$, $\hat{\gamma}_{ik} = u_i|a^{\mathrm{a}}_{ik}|/u$, $\hat{\beta}^{jl}_i = u_i|a^{\mathrm{o}}_{jl}|/u$, and $\hat{\delta}^{jl}_{ik} = u_i|a^{\mathrm{a}}_{ik}||a^{\mathrm{o}}_{jl}|/u$ and interaction parameters as $\hat{a}^{\mathrm{a}}_{ik} = \mathrm{sign}(a^{\mathrm{a}}_{ik})$ and $\hat{a}^{\mathrm{o}}_{jl} = \mathrm{sign}(a^{\mathrm{o}}_{jl})$. Parameters $\hat{\alpha}^l_i, \hat{\beta}^{jl}_i, \hat{\delta}^{jl}_{ik}, \hat{\gamma}_{ik} \geq 0$ capture the strength of interactions on communication and belief system graphs, and $\hat{a}^{\mathrm{a}}_{ik}, \hat{a}^{\mathrm{o}}_{jl} \in \{1, 0, -1\}$ capture connectivity and interaction signs. Equation 1 is

$$\dot{z}_{ij} = -d_{ij}z_{ij} + S\left(u\left(\hat{\alpha}^j_i z_{ij} + \sum_{\substack{k=1\\k\neq i}}^{N_{\mathrm{a}}} \hat{\gamma}_{ik}\hat{a}^{\mathrm{a}}_{ik}z_{kj} + \sum_{\substack{l\neq j\\l=1}}^{N_{\mathrm{o}}} \hat{\beta}^{jl}_i \hat{a}^{\mathrm{o}}_{jl}z_{il} + \sum_{\substack{k=1\\k\neq i}}^{N_{\mathrm{a}}}\sum_{\substack{l\neq j\\l=1}}^{N_{\mathrm{o}}} \hat{\delta}^{jl}_{ik}\hat{a}^{\mathrm{a}}_{ik}\hat{a}^{\mathrm{o}}_{jl}z_{kl}\right)\right) + b_{ij}. \qquad 14.$$

When $b_{ij} = 0$, the neutral state $\mathbf{z} = \mathbf{0}$ is an equilibrium for all values of $u$. The Jacobian matrix of the linearization of the dynamics about $\mathbf{z} = \mathbf{0}$ is

$$J(\mathbf{0}, u) = -\mathcal{D} + u\left(\mathcal{A} + (\hat{\Gamma} \odot \hat{A}_{\mathrm{a}}) \otimes \mathcal{I}_{N_{\mathrm{o}}} + \mathrm{diag}_i\{\hat{\mathcal{B}}_i \odot \hat{A}_{\mathrm{o}}\} + \hat{\Delta} \odot (\hat{A}_{\mathrm{a}} \otimes \hat{A}_{\mathrm{o}})\right), \qquad 15.$$

where $\mathcal{D} = \mathrm{diag}\{\mathbf{d}\} \in \mathbb{R}^{N_{\mathrm{a}}N_{\mathrm{o}} \times N_{\mathrm{a}}N_{\mathrm{o}}}$; $\mathcal{A} = \mathrm{diag}\{\hat{\boldsymbol{\alpha}}\} \in \mathbb{R}^{N_{\mathrm{a}}N_{\mathrm{o}} \times N_{\mathrm{a}}N_{\mathrm{o}}}$; $\mathcal{B}_i \in \mathbb{R}^{N_{\mathrm{o}} \times N_{\mathrm{o}}}$ is the matrix of weights $\hat{\beta}^{jl}_i$ for a given agent $i$; $\hat{\Delta} \in \mathbb{R}^{N_{\mathrm{a}}N_{\mathrm{o}} \times N_{\mathrm{a}}N_{\mathrm{o}}}$ is the matrix of weights $\hat{\delta}^{jl}_{ik}$ for a given agent $i$ and option $j$; $\hat{A}_{\mathrm{a}}$ and $\hat{A}_{\mathrm{o}}$ are the signed and unweighted adjacency matrices for the communication and belief system graphs, respectively; and $\odot$ is the Hadamard product.

Suppose $d_{ij} > 0$ for all $i,j$ and the matrix $\mathcal{A} + (\hat{\Gamma} \odot \hat{A}_{\mathrm{a}}) \otimes \mathcal{I}_{N_{\mathrm{o}}} + \mathrm{diag}_i\{\hat{\mathcal{B}}_i \odot \hat{A}_{\mathrm{o}}\} + \hat{\Delta} \odot (\hat{A}_{\mathrm{a}} \otimes \hat{A}_{\mathrm{o}})$ has at least one eigenvalue with positive real part. Then $J(\mathbf{0}, 0)$ has all eigenvalues with negative real part (indecision is stable), while $J(\mathbf{0}, u \to \infty)$ has at least one eigenvalue with positive real part (indecision is unstable). Thus, an indecision-breaking bifurcation must occur at a critical attention value $u = u^* > 0$.

Let $m$ be the number of eigenvalues of $J(\mathbf{0}, u^*)$ on the imaginary axis. Generically, $m = 1$ or $m = 2$ with a pair of complex conjugate eigenvalues.

If $m = 1$ and $S(\cdot)$ is odd, then generically the indecision-breaking bifurcation is a pitchfork bifurcation (top left diagram of **Figure 3*a***), and the critical subspace of $J(\mathbf{0}, u^*)$ is the span of its right null eigenvector $\mathbf{v}$, so $y = \langle \mathbf{v}, \mathbf{z}\rangle$. The span of the left null eigenvector $\mathbf{w}$ is the sensitivity subspace that determines the network response to small distributed inputs $b_{ij}$. If the opinion dynamics are monotone (67, 95), then $m = 1$. Monotonicity can be guaranteed in the case of structurally balanced network interactions (96–98).

For a network with no input, the bifurcation gives rise to two nonzero equilibria $\mathbf{z}^*_1(u)$ and $\mathbf{z}^*_2(u) = -\mathbf{z}^*_1(u)$ in a neighborhood of $u = u^*$, where $\langle \mathbf{v}, \mathbf{z}^*_1(u)\rangle > 0$ and $\langle \mathbf{v}, \mathbf{z}^*_2(u)\rangle < 0$. Whenever $\mathbf{b} \neq \mathbf{0}$ and $\langle \mathbf{w}, \mathbf{b}\rangle \neq \mathbf{0}$, the pitchfork bifurcation diagram unfolds, as in the top right diagram of **Figure 3*a***. In a neighborhood of $(\mathbf{z}, u) = (\mathbf{0}, u^*)$, the opinion dynamics have a unique, exponentially stable equilibrium $\mathbf{z}^*(u)$ that satisfies $\langle \mathbf{v}, \mathbf{z}^*(u)\rangle > 0\,(<0)$ whenever $b = \langle \mathbf{w}, \mathbf{b}\rangle > 0\,(<0)$. When $S$ is a perturbation of an odd sigmoid, the indecision-breaking bifurcation is an unfolding of the pitchfork exhibiting a transcritical bifurcation.

Including state-dependent attention as in Equation 2 with $\tau_u \to 0$, so that $u = u_0 + K_u \sum_{j=1}^{N_o} \sum_{k=1}^{N_a} a_{ik}^u (z_{kj})^2$, leaves unchanged the first- and second-order terms in the Lyapunov–Schmidt reduction and therefore also the critical and sensitivity subspaces that generically lead to an unfolded pitchfork. State-dependent attention, however, affects the nature of the pitchfork by inducing a change from supercritical to subcritical, as in the bottom diagrams of **Figure 3*a***. The subcritical pitchfork is associated with the emergence of network thresholds for opinion cascades with respect to the distributed input $b = \langle \mathbf{w}, \mathbf{b} \rangle$. Analysis and control of opinion cascades for complex attention networks, for different functional forms of the attention feedback term, and without the fast $\tau_u \to 0$ can be found in References 99 and 100.

If $m = 2$ and the leading eigenvalues of $J(\mathbf{0}, u)$ are a complex conjugate pair, a Hopf bifurcation occurs when indecision is broken. The critical eigenspace is then two-dimensional, and the bifurcation results in an oscillation. Unlike in the case of the pitchfork bifurcation, when distributed input aligned with the sensitivity subspace causes qualitative changes to the bifurcation diagram near the critical point, oscillations persist under perturbation and are qualitatively unchanged by small inputs to agents.

Characterizations of both the pitchfork and Hopf bifurcations have appeared in various works (36, 58, 91, 98, 99, 101–109) with varying assumptions about the structure of the communication and belief system networks and damping coefficients. In the cases studied, the critical and sensitivity subspaces of the bifurcation coincide with eigenspaces of standard graph matrices—e.g., the graph Laplacian $L$ (36, 91, 101–105) or communication adjacency matrix $A_a$ (98, 99, 106–108)—for two options and with the product of adjacency matrices of communication and belief system graphs $A_a \otimes A_o$ in the general case (58, 107–109). Understanding the resulting indecision-breaking bifurcation reduces to determining graph-theoretic conditions that ensure the critical subspace of the appropriate matrix has dimension one (pitchfork) or dimension two with a complex-conjugate pair of leading eigenvalues (Hopf). This is a dominance problem that can be addressed using Perron–Frobenius techniques for signed networks (68) (for a detailed analysis, see 109).

## 7. APPLICATIONS AND EXTENSIONS

### 7.1. Applications

The theory and models of fast and flexible multiagent decision-making reviewed in this article can be applied to investigate and design the dynamics of a wide range of groups in nature and technology that operate in the real world (see Section 1). For example, Leonard et al. (43) used the dynamics of Equation 3 to examine the historical asymmetry in polarization in the US Congress, where Republicans lean more strongly to the right than Democrats do to the left (dashed lines in **Figure 1*b***). Trends in ideological position were recovered (solid lines in **Figure 1*b***) using policy mood, a scalar measure of the mood of voters, to drive attention to self-reinforcing positive feedback. The dynamics were used by Park et al. (110) to explore the emergence of cooperation in repeated multiagent matrix games and by Musslick et al. (111) to investigate the stability–flexibility dilemma in cognitive control. The multioption dynamics are being used to generalize the study of spatial decision-making in animal groups (21, 24, 112).

Cathcart et al. (113) used these same dynamics to design and test, in experiments with human participants, social navigation strategies for a robot to move around oncoming human movers, where attention is driven by a distance to a collision. Hu et al. (114) used them in a closed loop with game-theoretic tools to resolve ambiguity in dynamic multiagent interactions, exemplified in a toll-booth coordination problem. An automatic procedure was provided for tuning the opinion dynamics as a function of game value functions, and an efficient trajectory planner was provided that computes agents' policies, guided by their evolving opinions such that coordination on tasks

emerges. Related approaches that leverage opinion dynamics for planning and control and automatically tune opinion dynamics based on physical system state are underway for car racing, task allocation, and other applications.

**Mixed-feedback loop:** a feedback loop in which negative and positive feedback coexist but are separated in range, timescale, or spatial scale

**Excitability:** the characteristic behavior of mixed-feedback systems in which negative and positive feedback are separated in timescale

**Action potential (or spike):** an excitable phenomenon responsible for pulsing electrical communication between neurons; it comprises a fast diverging phase ruled by fast positive feedback and a slow return to rest ruled by slow negative feedback

### 7.2. Extensions

Here we describe promising extensions of the theory and models described in this review.

**7.2.1. Continuous option spaces.** We have reviewed decision-making for a finite number of options, but certain contexts call for a continuum of options, such as in spatial navigation, where each option is a different heading direction. An extension can seamlessly be made to continuous option spaces using bifurcation theory for spatially extended systems.

**7.2.2. From fast and flexible to excitable decision-making.** Underlying fast and flexible decision-making is a mixed-feedback loop (115) arising from intertwined negative and positive feedback loops. Fast and flexible decision-making can be turned into excitability by adding an extra slower negative feedback loop, much in the same way as slow negative feedback currents terminate action potentials (or spikes) in neurons. As neurons have thresholds for action potential generation, excitable decision-makers have thresholds for decision generation. As neurons return to the excitable resting state after each action potential, excitable decision-makers return to the excitable neutral state after each decision. Enhanced flexibility in excitable decision-making comes from forgetting decisions and thus never getting stuck in a decision. The extension uses the interpretation of action potentials as one-option decisions to generalize to excitable multioption decision-making for a group of agents. The interpretation and generalization might also be important to recent neural code theories (116, 117), building on the role of single action potentials in the encoding of sensory, internal, decision, and motor information in patterns of neuronal activity.

## DISCLOSURE STATEMENT

The authors are not aware of any affiliations, memberships, funding, or financial holdings that might be perceived as affecting the objectivity of this review.

## ACKNOWLEDGMENTS

We acknowledge US Office of Naval Research grant N00014-19-1-2556 and US Army Research Office grant W911NF-18-1-0325.

## LITERATURE CITED

1. Ren W, Atkins E. 2007. Distributed multi-vehicle coordinated control via local information exchange. *Int. J. Robust Nonlinear Control* 17(10–11):1002–33
2. Rios-Torres J, Malikopoulos AA. 2016. Automated and cooperative vehicle merging at highway on-ramps. *IEEE Trans. Intell. Transp. Syst.* 18(4):780–89
3. Vilca J, Adouane L, Mezouar Y. 2018. Stable and flexible multi-vehicle navigation based on dynamic inter-target distance matrix. *IEEE Trans. Intell. Transp. Syst.* 20(4):1416–31
4. Fiorelli E, Leonard NE, Bhatta P, Paley DA, Bachmayer R, Fratantoni DM. 2006. Multi-AUV control and adaptive sampling in Monterey Bay. *IEEE J. Ocean. Eng.* 31(4):935–48
5. Leonard NE, Paley DA, Lekien F, Sepulchre R, Fratantoni DM, Davis RE. 2007. Collective motion, sensor networks, and ocean sampling. *Proc. IEEE* 95(1):48–74
6. Hu J, Niu H, Carrasco J, Lennox B, Arvin F. 2022. Fault-tolerant cooperative navigation of networked UAV swarms for forest fire monitoring. *Aerosp. Sci. Technol.* 123:107494
7. Liu Y, Nejat G. 2013. Robotic urban search and rescue: a survey from the control perspective. *J. Intell. Robot. Syst.* 72:147–65

8. Arnold RD, Yamaguchi H, Tanaka T. 2018. Search and rescue with autonomous flying robots through behavior-based cooperative intelligence. *J. Int. Humanit. Action* 3(1):18
9. Drew DS. 2021. Multi-agent systems for search and rescue applications. *Curr. Robot. Rep.* 2:189–200
10. Kolling A, Walker P, Chakraborty N, Sycara K, Lewis M. 2015. Human interaction with robot swarms: a survey. *IEEE Trans. Human-Mach. Syst.* 46(1):9–26
11. Wang X, Wang Y. 2017. Co-design of control and scheduling for human–swarm collaboration systems based on mutual trust. In *Trends in Control and Decision-Making for Human–Robot Collaboration Systems*, ed. Y Wang, F Zhang, pp. 387–413. Cham, Switz.: Springer
12. Ajoudani A, Zanchettin AM, Ivaldi S, Albu-Schäffer A, Kosuge K, Khatib O. 2018. Progress and prospects of the human–robot collaboration. *Auton. Robots* 42:957–75
13. Gerkey BP, Matarić MJ. 2004. A formal analysis and taxonomy of task allocation in multi-robot systems. *Int. J. Robot. Res.* 23(9):939–54
14. Korsah GA, Stentz A, Dias MB. 2013. A comprehensive taxonomy for multi-robot task allocation. *Int. J. Robot. Res.* 32(12):1495–512
15. Khamis A, Hussein A, Elmogy A. 2015. Multi-robot task allocation: a review of the state-of-the-art. In *Cooperative Robots and Sensor Networks*, ed. A Koubâa, J Martínez-de Dios, pp. 31–51. Cham, Switz.: Springer
16. Valentini G, Ferrante E, Dorigo M. 2017. The best-of-*n* problem in robot swarms: formalization, state of the art, and novel perspectives. *Front. Robot. AI* 4:9
17. Dörfler F, Chertkov M, Bullo F. 2013. Synchronization in complex oscillator networks and smart grids. *PNAS* 110(6):2005–10
18. Rinaldi S, Della Giustina D, Ferrari P, Flammini A, Sisinni E. 2016. Time synchronization over heterogeneous network for smart grid application: design and characterization of a real case. *Ad Hoc Netw.* 50:41–57
19. Chu CC, Iu HHC. 2017. Complex networks theory for modern smart grid applications: a survey. *IEEE J. Emerg. Sel. Top. Circuits Syst.* 7(2):177–91
20. Conradt L, Roper TJ. 2005. Consensus decision making in animals. *Trends Ecol. Evol.* 20(8):449–56
21. Couzin ID, Krause J, Franks NR, Levin SA. 2005. Effective leadership and decision-making in animal groups on the move. *Nature* 433(7025):513–16
22. Sumpter DJ, Krause J, James R, Couzin ID, Ward AJ. 2008. Consensus decision making by fish. *Curr. Biol.* 18(22):1773–77
23. Pagliara R, Gordon DM, Leonard NE. 2018. Regulation of harvester ant foraging as a closed-loop excitable system. *PLOS Comput. Biol.* 14(12):e1006200
24. Sridhar VH, Li L, Gorbonos D, Nagy M, Schell BR, et al. 2021. The geometry of decision-making in individuals and collectives. *PNAS* 118(50):e2102157118
25. Papadopoulou M, Fürtbauer I, O'Bryan LR, Garnier S, Georgopoulou DG, et al. 2023. Dynamics of collective motion across time and species. *Philos. Trans. R. Soc. B* 378(1874):20220068
26. Zeng L, Skinner SO, Zong C, Sippy J, Feiss M, Golding I. 2010. Decision making at a subcellular level determines the outcome of bacteriophage infection. *Cell* 141(4):682–91
27. Weitz JS, Mileyko Y, Joh RI, Voit EO. 2008. Collective decision making in bacterial viruses. *Biophys. J.* 95(6):2673–80
28. Balázsi G, Van Oudenaarden A, Collins JJ. 2011. Cellular decision making and biological noise: from microbes to mammals. *Cell* 144(6):910–25
29. Stewart I, Elmhirst T, Cohen J. 2003. Symmetry-breaking as an origin of species. In *Bifurcation, Symmetry and Patterns*, ed. J Buescu, SBSD Castro, AP da Silva Dias, IS Labouriau, pp. 3–54. Basel: Birkhäuser
30. Waters CM, Bassler BL. 2005. Quorum sensing: cell-to-cell communication in bacteria. *Annu. Rev. Cell Dev. Biol.* 21:319–46
31. Bogacz R. 2007. Optimal decision-making theories: linking neurobiology with behaviour. *Trends Cogn. Sci.* 11(3):118–25
32. Deco G, Rolls ET, Albantakis L, Romo R. 2013. Brain mechanisms for perceptual and reward-related decision-making. *Prog. Neurobiol.* 103:194–213
33. Suzuki S, Adachi R, Dunne S, Bossaerts P, O'Doherty JP. 2015. Neural mechanisms underlying human consensus decision-making. *Neuron* 86(2):591–602

34. Busemeyer JR, Gluth S, Rieskamp J, Turner BM. 2019. Cognitive and neural bases of multi-attribute, multi-alternative, value-based decisions. *Trends Cogn. Sci.* 23(3):251–63
35. Collins AG, Shenhav A. 2022. Advances in modeling learning and decision-making in neuroscience. *Neuropsychopharmacology* 47(1):104–18
36. Fontan A, Altafini C. 2021. A signed network perspective on the government formation process in parliamentary democracies. *Sci. Rep.* 11(1):5134
37. Siegenfeld AF, Bar-Yam Y. 2020. Negative representation and instability in democratic elections. *Nat. Phys.* 16(2):186–90
38. Bokhari A, Cliff D. 2022. Studying narrative economics by adding continuous-time opinion dynamics to an agent-based model of co-evolutionary adaptive financial markets. SSRN 4316574. **https://doi.org/10.2139/ssrn.4316574**
39. Zha Q, Kou G, Zhang H, Liang H, Chen X, et al. 2020. Opinion dynamics in finance and business: a literature review and research opportunities. *Financ. Innov.* 6:44
40. Morrison M, Kutz JN, Gabbay M. 2022. Transitions between peace and systemic war as bifurcations in a signed network dynamical system. *Netw. Sci.* 11(3):458–501
41. Baumann F, Lorenz-Spreen P, Sokolov IM, Starnini M. 2020. Modeling echo chambers and polarization dynamics in social networks. *Phys. Rev. Lett.* 124(4):048301
42. Santos FP, Lelkes Y, Levin SA. 2021. Link recommendation algorithms and dynamics of polarization in online social networks. *PNAS* 118(50):e2102141118
43. Leonard NE, Lipsitz K, Bizyaeva A, Franci A, Lelkes Y. 2021. The nonlinear feedback dynamics of asymmetric political polarization. *PNAS* 118(50):e2102149118
44. Gajewski ŁG, Sienkiewicz J, Hołyst JA. 2022. Transitions between polarization and radicalization in a temporal bilayer echo-chamber model. *Phys. Rev. E* 105(2):024125
45. Levin SA, Weber EU. 2023. Polarization and the psychology of collectives. *Perspect. Psychol. Sci.* **https://doi.org/10.1177/17456916231186614**
46. Leung HCH, Li Z, She B, Paré PE. 2023. Leveraging opinions and vaccination to eradicate networked epidemics. In *2023 European Control Conference*. Piscataway, NJ: IEEE. **https://doi.org/10.23919/ECC57647.2023.10178234**
47. Yanga L, Constantino SM, Grenfell BT, Weber EU, Levin SA, Vasconcelos VV. 2022. Sociocultural determinants of global mask-wearing behavior. *PNAS* 119(41):e2213525119
48. Constantino SM, Weber EU. 2021. Decision-making under the deep uncertainty of climate change: the psychological and political agency of narratives. *Curr. Opin. Psychol.* 42(41):151–59
49. Converse PE. 2006. The nature of belief systems in mass publics (1964). *Crit. Rev.* 18(1–3):1–74
50. Seeley TD, Passino K, Visscher K. 2006. Group decision making in honey bee swarms. *Am. Sci.* 94(3):220–29
51. Seeley TD, Visscher PK, Schlegel T, Hogan PM, Franks NR, Marshall JAR. 2012. Stop signals provide cross inhibition in collective decision-making by honeybee swarms. *Science* 335(6064):108–11
52. Guckenheimer J, Holmes P. 1983. *Nonlinear Oscillations, Dynamical Systems, and Bifurcations of Vector Fields*. New York: Springer
53. Golubitsky M, Schaeffer DG. 1985. *Singularities and Groups in Bifurcation Theory*. New York: Springer
54. Strogatz S. 1994. *Nonlinear Dynamics and Chaos*. Boca Raton, FL: CRC
55. Golubitsky M, Stewart I, Shaeffer D. 1988. *Singularities and Groups in Bifurcation Theory*, Vol. 2. New York: Springer
56. Golubitsky M, Stewart I. 2002. *The Symmetry Perspective*. Basel: Birkhäuser
57. Elmhirst T. 2004. $S_N$-equivariant symmetry-breaking bifurcations. *Int. J. Bifurc. Chaos* 14(3):1017–36
58. Franci A, Golubitsky M, Stewart I, Bizyaeva A, Leonard NE. 2023. Breaking indecision in multiagent, multioption dynamics. *SIAM J. Appl. Dyn. Syst.* 22(3):1780–817
59. Golubitsky M, Stewart I. 2023. *Dynamics and Bifurcation in Networks: Theory and Applications of Coupled Differential Equations*. Philadelphia: Soc. Ind. Appl. Math.
60. Wilson HR, Cowan JD. 1972. Excitatory and inhibitory interactions in localized populations of model neurons. *Biophys. J.* 12(1):1–24
61. Wilson HR, Cowan JD. 1973. A mathematical theory of the functional dynamics of cortical and thalamic nervous tissue. *Kybernetik* 13(2):55–80

62. Hopfield JJ. 1982. Neural networks and physical systems with emergent collective computational abilities. *PNAS* 79(8):2554–58
63. Hopfield JJ. 1984. Neurons with graded response have collective computational properties like those of two-state neurons. *PNAS* 81(10):3088–92
64. Hodgkin AL, Huxley AF. 1952. A quantitative description of membrane current and its application to conduction and excitation in nerve. *J. Physiol.* 117(4):500–44
65. Dalege J, Galesic M, Olsson H. 2023. Networks of beliefs: an integrative theory of individual-and social-level belief dynamics. OSF Preprints 368jz. **https://doi.org/10.31219/osf.io/368jz**
66. Gardner TS, Cantor CR, Collins JJ. 2000. Construction of a genetic toggle switch in *Escherichia coli*. *Nature* 403(6767):339–42
67. Smith HL. 2008. *Monotone Dynamical Systems: An Introduction to the Theory of Competitive and Cooperative Systems*. Providence, RI: Am. Math. Soc.
68. Elhashash A, Szyld D. 2008. On general matrices having the Perron-Frobenius property. *Electron. J. Linear Algebra* 17:389–413
69. DeGroot MH. 1974. Reaching a consensus. *J. Am. Stat. Assoc.* 69(345):118–21
70. Abelson RP. 1964. Mathematical models of the distribution of attitudes under controversy. In *Contributions to Mathematical Psychology*, ed. N Frederiksen, H Gulliksen, pp. 142–60. New York: Holt, Rinehart, & Winston
71. Olfati-Saber R, Fax JA, Murray RM. 2007. Consensus and cooperation in networked multi-agent systems. *Proc. IEEE* 95(1):215–33
72. Garin F, Schenato L. 2010. A survey on distributed estimation and control applications using linear consensus algorithms. In *Networked Control Systems*, ed. A Bemporad, M Heemels, M Johansson, pp. 75–107. London: Springer
73. Cao Y, Yu W, Ren W, Chen G. 2012. An overview of recent progress in the study of distributed multi-agent coordination. *IEEE Trans. Ind. Inform.* 9(1):427–38
74. Qin J, Ma Q, Shi Y, Wang L. 2016. Recent advances in consensus of multi-agent systems: a brief survey. *IEEE Trans. Ind. Electron.* 64(6):4972–83
75. Mei W, Bullo F, Chen G, Hendrickx JM, Dörfler F. 2022. Micro-foundation of opinion dynamics: rich consequences of the weighted-median mechanism. *Phys. Rev. Res.* 4(2):023213
76. Friedkin NE, Johnsen EC. 1990. Social influence and opinions. *J. Math. Sociol.* 15(3–4):193–206
77. Friedkin NE, Johnsen EC. 1999. Social influence networks and opinion change. In *Advances in Group Processes*, Vol. 16, ed. SR Thye, EJ Lawler, MW Macy, HA Walker, pp. 1–29. Stamford, CT: JAI
78. Friedkin NE, Bullo F. 2017. How truth wins in opinion dynamics along issue sequences. *PNAS* 114(43):11380–85
79. Parsegov SE, Proskurnikov AV, Tempo R, Friedkin NE. 2017. Novel multidimensional models of opinion dynamics in social networks. *IEEE Trans. Autom. Control* 62(5):2270–85
80. Jia P, MirTabatabaei A, Friedkin NE, Bullo F. 2015. Opinion dynamics and the evolution of social power in influence networks. *SIAM Rev.* 57(3):367–97
81. Friedkin NE. 2011. A formal theory of reflected appraisals in the evolution of power. *Adm. Sci. Q.* 56:501–29
82. Altafini C. 2013. Consensus problems on networks with antagonistic interactions. *IEEE Trans. Autom. Control* 58(4):935–46
83. Proskurnikov AV, Matveev AS, Cao M. 2015. Opinion dynamics in social networks with hostile camps: consensus versus polarization. *IEEE Trans. Autom. Control* 61(6):1524–36
84. Zhang H, Chen J. 2017. Bipartite consensus of multi-agent systems over signed graphs: state feedback and output feedback control approaches. *Int. J. Robust Nonlinear Control* 27(1):3–14
85. Hegselmann R, Krause U. 2002. Opinion dynamics and bounded confidence models, analysis, and simulations. *J. Artif. Soc. Soc. Simul.* 5(3):121–32
86. Lorenz J. 2006. Continuous opinion dynamics of multidimensional allocation problems under bounded confidence: More dimensions lead to better chances for consensus. *Eur. J. Econ. Soc. Syst.* 19:213–27
87. Dandekar P, Goel A, Lee DT. 2013. Biased assimilation, homophily, and the dynamics of polarization. *PNAS* 110(15):5791–96

88. Xia W, Ye M, Liu J, Cao M, Sun XM. 2020. Analysis of a nonlinear opinion dynamics model with biased assimilation. *Automatica* 120:109113
89. Pais D, Hogan PM, Schlegel T, Franks NR, Leonard NE. 2013. A mechanism for value-sensitive decision-making. *PLOS ONE* 8(9):e73216
90. Reina A, Marshall JA, Trianni V, Bose T. 2017. Model of the best-of-*N* nest-site selection process in honeybees. *Phys. Rev. E* 95(5):052411
91. Gray R, Franci A, Srivastava V, Leonard NE. 2018. Multiagent decision-making dynamics inspired by honeybees. *IEEE Trans. Control Netw. Syst.* 5(2):793–806
92. Usher M, McClelland JL. 2001. The time course of perceptual choice: the leaky, competing accumulator model. *Psychol. Rev.* 108(3):550–92
93. Brown E, Holmes P. 2001. Modeling a simple choice task: stochastic dynamics of mutually inhibitory neural groups. *Stochast. Dyn.* 1(2):159–91
94. Bogacz R, Usher M, Zhang J, McClelland JL. 2007. Extending a biologically inspired model of choice: multi-alternatives, nonlinearity and value-based multidimensional choice. *Philos. Trans. R. Soc. B* 362(1485):1655–70
95. Angeli D, Sontag ED. 2003. Monotone control systems. *IEEE Trans. Autom. Control* 48(10):1684–98
96. Sontag ED. 2007. Monotone and near-monotone biochemical networks. *Syst. Synth. Biol.* 1(2):59–87
97. Altafini C. 2012. Dynamics of opinion forming in structurally balanced social networks. *PLOS ONE* 7(6):e38135
98. Bizyaeva A, Amorim G, Santos M, Franci A, Leonard NE. 2022. Switching transformations for decentralized control of opinion patterns in signed networks: application to dynamic task allocation. *IEEE Control Syst. Lett.* 6:3463–68
99. Bizyaeva A, Sorochkin T, Franci A, Leonard NE. 2021. Control of agreement and disagreement cascades with distributed inputs. In *2021 60th IEEE Conference on Decision and Control*, pp. 4994–99. Piscataway, NJ: IEEE
100. Franci A, Bizyaeva A, Park S, Leonard NE. 2021. Analysis and control of agreement and disagreement opinion cascades. *Swarm Intell.* 15:47–82
101. Qin J, Fu W, Zheng WX, Gao H. 2016. On the bipartite consensus for generic linear multiagent systems with input saturation. *IEEE Trans. Cybernet.* 47(8):1948–58
102. Franci A, Srivastava V, Leonard NE. 2015. A realization theory for bio-inspired collective decision-making. arXiv:1503.08526 [math.OC]
103. Gray R, Franci A, Srivastava V, Leonard NE. 2017. An agent-based framework for bio-inspired, value-sensitive decision-making. *IFAC-PapersOnLine* 50(1):8238–43
104. Abara PU, Ticozzi F, Altafini C. 2017. Spectral conditions for stability and stabilization of positive equilibria for a class of nonlinear cooperative systems. *IEEE Trans. Autom. Control* 63(2):402–17
105. Fontan A, Altafini C. 2017. Multiequilibria analysis for a class of collective decision-making networked systems. *IEEE Trans. Control Netw. Syst.* 5(4):1931–40
106. Bizyaeva A, Matthews A, Franci A, Leonard NE. 2021. Patterns of nonlinear opinion formation on networks. In *2021 American Control Conference*, pp. 2739–44. Piscataway, NJ: IEEE
107. Bizyaeva A, Franci A, Leonard NE. 2022. Nonlinear opinion dynamics with tunable sensitivity. *IEEE Trans. Autom. Control* 68(3):1415–30
108. Bizyaeva A, Franci A, Leonard NE. 2023. Sustained oscillations in multi-topic belief dynamics over signed networks. In *2023 American Control Conference*, pp. 4296–301. Piscataway, NJ: IEEE
109. Bizyaeva A, Franci A, Leonard NE. 2023. Multi-topic belief formation through bifurcations over signed social networks. arXiv:2308.02755 [physics.soc-ph]
110. Park S, Bizyaeva A, Kawakatsu M, Franci A, Leonard NE. 2022. Tuning cooperative behavior in games with nonlinear opinion dynamics. *IEEE Control Syst. Lett.* 6:2030–35
111. Musslick S, Bizyaeva A, Agaron S, Leonard NE, Cohen JD. 2019. Stability-flexibility dilemma in cognitive control: a dynamical system perspective. In *Proceedings of the 41st Annual Meeting of the Cognitive Science Society*, pp. 2420–26. Seattle, WA: Cogn. Sci. Soc.
112. Nabet B, Leonard NE, Couzin ID, Levin SA. 2009. Dynamics of decision making in animal group motion. *J. Nonlinear Sci.* 19:399–435

113. Cathcart C, Santos M, Park S, Leonard NE. 2023. Proactive opinion-driven robot navigation around human movers. In *2023 IEEE/RSJ International Conference on Intelligent Robots and Systems*. Piscataway, NJ: IEEE. Forthcoming
114. Hu H, Nakamura K, Hsu KC, Leonard NE, Fisac JF. 2023. Emergent coordination through game-induced nonlinear opinion dynamics. In *2023 IEEE 62nd Conference on Decision and Control*. Piscataway, NJ: IEEE. Forthcoming
115. Sepulchre R, Drion G, Franci A. 2019. Control across scales by positive and negative feedback. *Annu. Rev. Control Robot. Auton. Syst.* 2:89–113
116. Douglas R, Martin K. 2007. Mapping the matrix: the ways of neocortex. *Neuron* 56(2):226–38
117. Riquelme JL, Hemberger M, Laurent G, Gjorgjieva J. 2023. Single spikes drive sequential propagation and routing of activity in a cortical network. *eLife* 12:e79928